A thesis presented to the Faculty of Science in partial fulfillment of the requirements for the degree

Master of Science in Physics, Biophysics specialization

Study of three-dimensional bacterial colonies: how expression of motility and adhesion factors control colony morphology

Mireia Cordero Sánchez

`xjl924@alumni.ku.dk`

Supervisors: Liselotte Jauffred & Namiko Mitarai

May 2021

To my dad, who was often in my thoughts during this journey

ACKNOWLEDGEMENTS

First and foremost I would like to thank my supervisors Liselotte Jauffred and Namiko Mitarai for their invaluable advice, suggestions and support during this masters thesis. I would also like to thank Stanley Brown for discussing and explaining to me numerous phenomena that as a physicist I was not aware of. A special thanks to my fellow teammates Alba García Vázquez and Martin Møller Larsen who have assisted me in a variety of aspects, from providing interesting bibliography to their immense cooperation in the lab. I also appreciate the help from the whole Biocomplexity group and Experimental Biophysics group whose weekly meetings made easier to work in this pandemic times. I am grateful for the support given by my family and friends not only this last months but during all my academic years. Lastly, I specially want to thank Albert that apart from giving me coding tips has patiently listened to all the daily struggles an experimental research involves.

ABSTRACT

The morphology of bacterial colonies can provide plenty of information about how the cells adapt and overcome different changes in the environment. In this project, a novel approach to study three-dimensional bacterial colonies by growing them in semi-solid media is proposed. The colonies are later imaged and quantified, allowing a comparison between morphologies of multiples bacterial strains whose main difference is the deletion of structures responsible of adhesion and motility processes. After growing the bacterial strains in different conditions, diverse phenomena are observed such as more elongated colony shapes as the stiffness of the media increases or the appearance of microcolonies around a main colony for motile strains growing at 0.5% agar concentration. The later being reproduced with a modification to the Eden growth model, known to describe the formation of specific types of clusters such as bacterial colonies. Overall, with the experimental techniques employed, the morphological differences observed seem to have a greater dependence with the environmental conditions rather than with the structures deleted in the strains.

CONTENTS

Appendices

LIST OF FIGURES

LIST OF TABLES

A B B R E V I A T I O N S

WT MS613, MG1655 K-12 reference (F-lambda- ilvG- rfb-50 rph-1) strain

ΔfliC NM109, MG1655fliC::kan strain

Δflu MS427, MG1655Δflu strain

Δfim MS428, MG1655Δfim strain

ΔfluΔfim MS528, MG1655ΔfluΔfim strain

YFP Yellow Fluorescent Protein

CFP Cyan Fluorescent Protein

GLCM Grey level co-occurrence matrix

LB Lysogeny broth, rich media

MM M63 Minimal media

MMCA M63 Minimal media suplemented with casamino acids

CLSM Confocal Laser Scanner Microscopy

FD Fractal dimension

AR Aspect ratio

OD600 Optical density of a sample measured at a wavelength of 600 nm

IPTG Isopropyl β-d-1-thiogalactopyranoside

1

INTRODUCTION

Bacteria are single celled microbes that can be found in almost every habitat on Earth. They reproduce by binary fission, a process where a bacterium divides into two identical cells. In general, in in vitro experiments bacteria grow on top of solid media where they form colonies, a mass of microorganisms originating from a single or few cells. The colonies can present different forms, elevations or margins. The colony morphology is frequently used by the scientific and clinical communities as an auxiliary mean to identify bacterial species, because of their different and specific growth patterns [1],[2]. The question of why the shape of the colonies changes, has been gaining attention recently because it is thought to be an expression of how bacteria adapt to different environments [3]. However, many of the studies focus on two-dimensional colonies. There is plenty of experimental data sets and mathematical models about them [4].

New research lines study how this two-dimensional colonies become three-dimensional [5], since these results can have an important impact on the understanding of biofilms. A biofilm is a complex three-dimensional microbial association, that may be formed by multiple or single microbial species, anchored to surfaces [6]. The cells on it are protected against many environmental stresses, such as antibiotics, and these structures are considered to be responsible for 65% of bacterial infections [7].

Understanding how bacteria from single species form colonies in three dimensions will be an enormous step in the right direction to the description of even more complex phenomena. One of the first things that can be studied is the morphology of the colony, which is still unknown.

The aim of this thesis is to study the morphology of *E.coli* colonies growing in three dimensions. To do so, an experimental data set is required. The colonies can be formed by growing single cells inside a semi-solid media to later be imaged with a confocal microscope. Once the experimental images are obtained parameters to quantify the differences between morphologies will be proposed.

Considering that the shape of the colony contains a lot of information, different bacterial strains will be grown and quantified. More precisely, the bacterial strains studied present deletions of different structures found on the bacterial surface that are related to bacterial motility and adhesion processes. Additionally, a reproduction of the experimental results will be attempted by modifying a theoretical framework, the Eden growth model, used to describe the growth of specific types of clusters such as bacterial colonies [8].

1.1 THESIS OUTLINE

This thesis starts with an overview of the biological system studied in Chapter 2. This is followed by a briefly presentation of the imaging systems used to recollect the experimental data in Chapter 3 and a description of the parameters chosen to quantify the different colony morphologies in Chapter 4. Chapter 5 explains the experimental methods followed and the results of these are presented and discussed in Chapter 6. Chapter 7, which gives an outline of the mathematical model used to obtain in silico results comes next. The results of this are seen and discussed in Chapter 8. Finally the conclusions and future work are described in Chapter 9.

BIOLOGICAL BACKGROUND

Bacteria are prokaryotic microorganisms that appear in different sizes, usually between $0.5 \ \mu m$ and $5 \ \mu m$, and shapes such as spheres, filaments or rods. They are the most abundant organism on Earth and can be found almost everywhere including extreme environments as hot springs or even radioactive waste [9]. Bacteria are important in numerous industrial processes as the production of aliments and medicines. Even though in the human body most of the bacteria are harmless or involved in beneficial processes, some pathogenic bacteria can cause infectious illness, in many of these infections bacteria organise as biofilms.

Bacteria reproduce by binary fission, before dividing bacteria have to grow. They do so by a complex process involving numerous reactions. If bacteria grow under ideal conditions, such as a homogeneous rich medium, they can divide in the time scale of minutes. However, in heterogeneous environments with poor nutritional levels the division is suggested to occur as slowly as years [10]. Under controlled conditions, bacteria can grow as a batch culture where they have a fixed amount of food provided by a liquid medium. In a batch culture bacteria experience four different growth phases. The first one is the lag phase where the growth is essentially zero, it finishes when the initial population doubles and its length can vary. The second phase is the exponential one, cell growth is the fastest possible. In this phase the doubling time, time it takes for a cell division to occur, of the bacteria can be computed. When there is no net growth in the culture the stationary phase begins. In this third phase cells still grow and divide but the number of new cells it is balanced with the number of cells dying. The final phase of bacterial growth is the death phase, characterized by a net loss of viable cells. Real systems do not have to follow the previous phases, figure 1. For example, bacteria growing in colonies may compete for local resources. To know how bacteria grow in three-dimensional colonies is one of the reasons that makes the understanding of the colony geometry relevant.
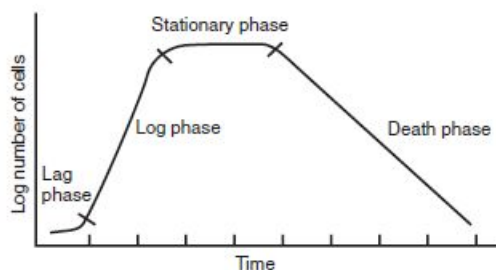
Figure 1: Bacterial growth curve in a batch culture. The four different phases can be appreciated by the comparison between number of cells in the culture, in logarithmic scale, over time. Image from [11].

2.1 BACTERIAL MOTILITY

Bacterial motility is a process where bacteria can move by their own means by expending energy. It is the key to the emergence of several biological phenomena such as biofilm formation. Bacteria can move through liquids or over moist surfaces by a wide range of mechanisms [12], that can be seen in figure 2:

- Swimming: Individual movement where planktonic bacteria rotate its helical flagella to create a thrust force that moves them forwards in liquid media [13].

- Swarming: Multicellular and rapid movement of a bacterial population across solid or semi-solid surfaces powered by rotating helical flagella. Leads to bacterial migration in groups of tightly bound cells. It is dependent on the ability of surface-adhering bacteria to undergo a differentiation process characterized by the production of specialized swarm cells [14].

- Twitching: Form of crawling bacterial motility used to move over surfaces powered by the extension and retraction of pili. It is required to form microcolonies in young biofilms [15].

- Gliding: Movement independent of propulsive structures such as flagella or pili that involves focal adhesion complexes. It allows bacteria to move over surfaces and along surface of low aqueous films [16].

- Sliding: Passive surface translocation powered by the pushing force of dividing cells and facilitated by a surfactant [17].
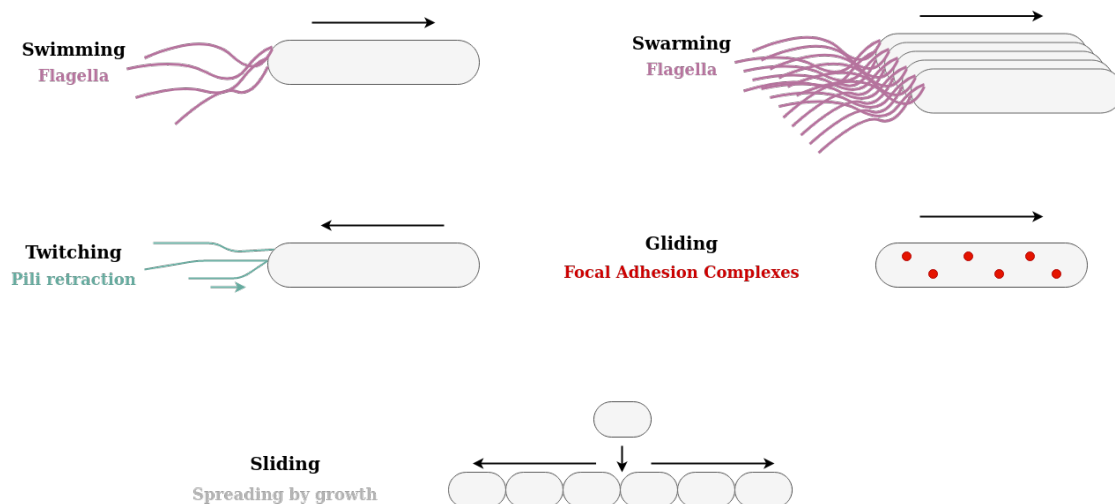
Figure 2: Schematic representation of the mechanisms behind bacterial motility. The direction of movement is indicated by black arrows and the responsible structures as coloured elements.

Regardless the motility type, bacteria react to stimuli using complex sensory systems that allow them to move to the most optimal environment. How most of the motility mechanisms work remains unknown and most of the studies focus on bacterial movement over surfaces. On this thesis we have the opportunity of gain some knowledge whether some of the processes will occur when colonies are formed in a semi-solid media.

2.2   ESCHERICHIA COLI

Escherichia coli was the bacteria chosen for this project. It is a coliform bacteria that in its natural habitat lives in the digestive track of healthy mammals. There are pathogenic strains that colonize healthy organisms and produce infections of different severity [18].

For growing inside solid media we work with *Escherichia coli K-12* [19], that was first isolated from the stool of a convalescent diphtheria patient in California, since it is a well studied model system. It is usually used in laboratories because it functions well. It has a short generation time and low nutritional requirements, making its growth robust in different media. *E.coli* grows optimally at 37ºC and can live in a petri dish for several weeks. This bacterium genome is well understood, this allows to perform modifications to it in an easy way with the help of bacteriophages or plasmids.

IMAGING THREE DIMENSIONAL COLONIES

When studying biological structures three-dimensional imaging is often required for its depth information. Optical sectioning microscopy generates two-dimensional images stacked to form a volume and allows us to image biological systems in good physiological conditions [20]. Lightsheet microscopes and confocal microscopes are some of the available optical sectioning devices, these provide powerful means to eliminate the background caused by out-of-focus fluorescent light.

3.1 FLUORESCENCE IMAGING

Fluorescence microscopy is based on a variety of fluorescent probes that specifically target molecules or cells. Fluorescence emission occurs when a fluorescent molecule absorbs light of a certain excitation wavelength [21]. This light absorption excites the fluoropohore to an unstable state and when it decays back to its ground state a fluorescent light of a specific wavelength is emitted.

This process can be visualized via a Jablonski diagram in figure 3A. A photon of a certain energy, $h\nu$, excites electrons from their ground molecular orbital state to a higher unoccupied molecular orbital. After absorbing energy from the excitation light, the electron is first relaxed by a non-radiative process to one of the lower vibrational sublevels. Then, the electron relaxes back to its ground state by emitting a photon of a certain energy $h\nu'$. This emitted light is what is called fluorescence. Due to the dissipation of energy the emitted photon has a lower energy than the incident photon ($h\nu > h\nu'$) producing a shift in the wavelength that allows the use of fluorescence to image different systems. Therefore, a fluorescent molecule has two important spectra, illustrated in figure 3B. Its emission spectra gives the probability a molecule will emit a certain wavelength and the excitation spectra gives the probability that a molecule will be excited by a light of specific wavelength. Both spectra present an absolute maximum and the distance between them is known as Stokes shift. To make the detection of fluorescence easier it is important to work with fluorophores with a big enough Stokes shift .

 A common problem of fluorescence microscopy is photo bleaching, an alteration of a fluorophore molecule such that it can no longer be detected because it is unable to fluoresce permanently. It can happen due to long exposure of a sample or exposition to a very high intensity light.

A

B
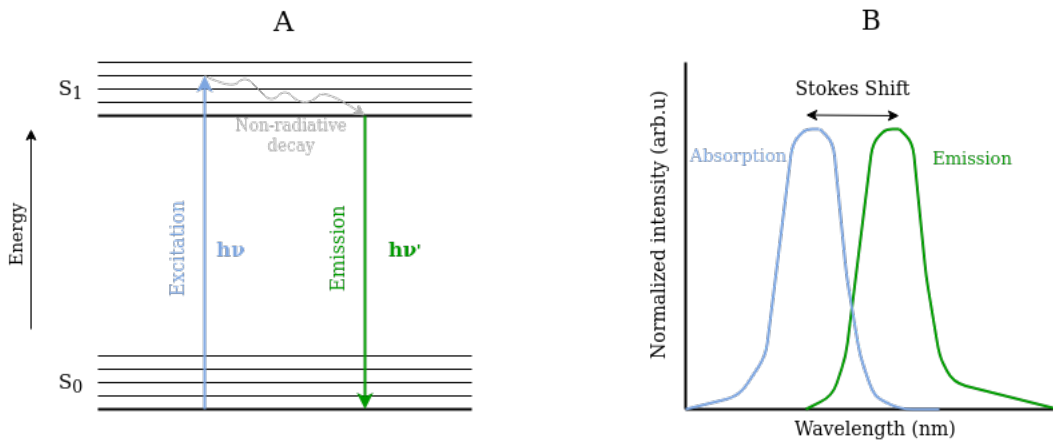
Figure 3: (a) Jablonski diagram illustrating the energy state transitions leading to a non-radiative decay and the subsequent emission of fluorescence. (b) Example of excitation and emission spectra for a fluorophore. The excitation range can be seen in blue and the emission in green. The Stokes shift between maximums it is also included.

3.2 CONFOCAL MICROSCOPY

Confocal microscopy is an excellent tool for making measurements in cells, when used appropriately allows fluorescence quantification with high spatial precision.

Confocal microscopes aim to overcome limitations of traditional wide-field fluorescence microscopes. It uses point illumination and a pinhole to eliminate out-of-focus signal [22]. Since only fluorescence really close to the focal plane can be detected the image's optical resolution increases at cost of a decreased signal intensity.

The confocal features are shown in figure 4. A coherent light emitted by the laser system acts as the excitation source. This laser passes through a pinhole aperture situated in a confocal plane with a second pinhole in front of the detector and a scanning point on the specimen. Then, the light is reflected by a dichromatic mirror and scanned across the sample in a certain focal plane. A secondary fluorescence emitted from points on the specimen pass back through the dichromatic mirror and are focused as a confocal point at the detector pinhole aperture creating a two-dimensional image [23]. Scanning through a range of focal planes allows for the reconstruction of a three dimensional image.

In this thesis the bacterial colonies are imaged with confocal microscopy techniques. These were chosen after considering relevant factors in the obtainment of images.

The objective lens used determines the overall resolution of the system. Resolution in optical systems is commonly accepted to be the minimum separation distance between two sample features that enables them to be distinguished as separate in the final image. It can be quantified as a function of the light wavelength (λ) and the numerical aperture (NA) of the optical system. The numerical aperture is defined as the half angle of the cone of light focused or collected by the objective (θ) and the refractive index n of the mounting medium:

$$NA = n \cdot sin(\theta) \tag{1}$$
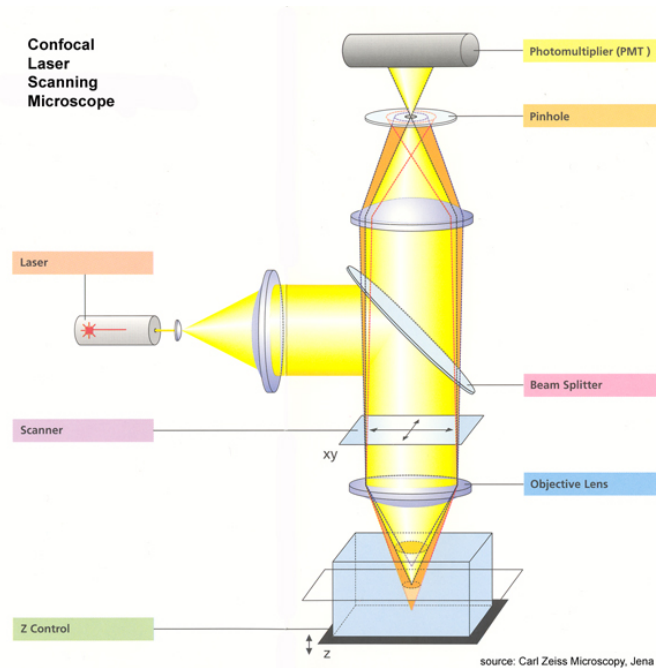
Figure 4: Schematics of the elements in Confocal Laser Scanning Microscopes. The laser beam passing through a light source aperture can be seen. This is then focused into a small area on the surface of the sample by an objective lens. The images of are built up pixel-by pixel by collecting the photons emitted from the sample fluorophores. Image from [24].

The Rayleigh criterion is a rule of thumb to estimate the smallest lateral resolution [22]. It considers two identical points to be barely discernible when they are separated by:

$$d = 1.22 \cdot \frac{\lambda}{2 \cdot NA} \tag{2}$$

Another important factor is the penetration depth. It is a measure of how deep light or any electromagnetic radiation can penetrate into a material. Due to absorption and scattering, penetration depth is generally limited to 50–100 μm for confocal microscopes.

Resolution and penetration depth are magnitudes dependent on each other since a higher numerical aperture increases the resolution of the system but at the same time limits the depth at which the sample can be imaged. That is because a bigger NA decreases the distance from the objective lens to the surface of the plate of the sample.

Confocal microscopy provides a better resolution and penetration depth compared to other optical sectioning techniques, but it is slower, making it less suitable to live-cell imaging. In this study we focus in the morphology of bacterial colonies, and this is not likely to change during the pixel-by-pixel image reconstruction, so CLSM is the best option for this project.

COLONY QUANTIFICATION

Multiple parameters can be extracted from experimental data. To quantify the colonies formed in semi-solid media I considered some three dimensional structural parameters commonly used to classify other biological data sets such as biofilms [25]. Although the definition of the quantities is relatively straight forward interpret the results of those is not trivial.

The parameters can be classified in two categories, Textural or Volumetric parameters [26].

4.1 TEXTURAL PARAMETERS

The texture is defined as the appearance, or consistency of a surface or substance. In an image, can be described as a repeating pattern of local variations in its intensity and provides information about spatial distribution of intensity levels in a vicinity.

Textural parameters quantify the structure of the colony by comparing visual components, all of them are obtained from the grey level co-occurrence matrix (GLCM) [27]. GLCM is a matrix with number of rows and columns equal to the number of grey levels, in 8-bit images goes from $(0, 255)$, and shows how often pairs of pixels with specific values and in a specified spatial relationship occur in an image. In three dimensions the GLCM is obtained from the spatial dependence matrix in each of the directions. In the X direction the spatial dependence matrix is defined as:

$$P_X = \{P_x(a,b)\} = \begin{bmatrix} P_x(0,0) & P_x(0,1) & \dots & P_x(0,255) \\ P_x(1,0) & P_x(1,1) & \dots & P_x(1,255) \\ \vdots & \vdots & \ddots & \vdots \\ P_x(255,0) & P_x(255,1) & \dots & P_x(255,255) \end{bmatrix} \tag{3}$$

Where $P_x(a,b)$ is the number of times the grey level changes from $a \rightarrow b$ in the X direction between neighboring pixels for all the image stacks. In the Y and Z directions the spatial dependence matrix is computed in an equivalent way.

$$P_Y = \{P_Y(a,b)\} = \begin{bmatrix} P_Y(0,0) & P_Y(0,1) & \dots & P_Y(0,255) \\ P_Y(1,0) & P_Y(1,1) & \dots & P_Y(1,255) \\ \vdots & \vdots & \ddots & \vdots \\ P_Y(255,0) & P_Y(255,1) & \dots & P_Y(255,255) \end{bmatrix} \tag{4}$$

$$P_Z = \{P_Z(a,b)\} = \begin{bmatrix} P_Z(0,0) & P_Z(0,1) & \ldots & P_Z(0,255) \\ P_Z(1,0) & P_Z(1,1) & \ldots & P_Z(1,255) \\ \vdots & \vdots & \ddots & \vdots \\ P_Z(255,0) & P_Z(255,1) & \ldots & P_Z(255,255) \end{bmatrix} \tag{5}$$

The GLCM is computed by normalizing the spatial dependence matrix, which is a sum of the three dependence matrix directions $P_{XYZ} = P_X + P_Y + P_z$, by dividing it by the sum of all the counts:

$$[GLCM] = \frac{[P_{XYZ}]}{\sum P_{XYZ}} = [P_N] \tag{6}$$

In this study three textural parameters will be computed from the GLCM.

4.1.1   *Homogeneity*

The textural homogeneity measures similarity of image structures that are close in space. It is normalized with respect to the distance between changes in texture. The bigger the value the more homogeneous is the image structure. Can be computed as:

$$H = \sum_{1}^{N_a}\sum_{1}^{N_b} \frac{1}{1 + (a-b)^2} \cdot P_N(a,b) \tag{7}$$

From the expression we can see that changes in neighbouring pixels with big differences in its grey level number contribute less to it than changes in neighbouring pixels with smaller transitions in their grey level values.

4.1.2   *Textural Entropy*

The textural entropy is a measure of randomness in the grey scale values of the image. The higher the textural entropy, the more heterogeneous is the image. Can be computed as:

$$TE = -\sum_{1}^{N_a}\sum_{1}^{N_b} P_N(a,b) \cdot \ln(P_N(a,b)) \tag{8}$$

For completely uniform images the textural entropy becomes zero.

4.1.3   *Energy*

The textural energy is a measure of regularity in patterns of pixels and it is sensitive to the similarity of their shapes and the orientation of the clusters. A small energy value indicates that repeated patters of pixels clusters are frequent while a higher value means a more homogeneous image without repeated patterns. Can be computed as:

$$E = \sum_{1}^{N_a}\sum_{1}^{N_b} P_N(a,b)^2 \tag{9}$$

4.1.4 *Example*

All this parameters can be better understood with a simple example. In the figure 5A, we have a completely white image meaning that the textural entropy will equal zero and both the energy and homogeneity equal one. In an image with a single element, 5B, the entropy increases and both the energy and homogeneity start decreasing. Since the definitions of energy and homogeneity are quite similar the difference between them can be clearly seen when looking at figures 5C and 5D. Image 5C incorporates an additional cluster shifted vertically, consequently there is a pattern of repeating clusters in the vertical direction but the shapes of the two clusters are the same, meaning that the energy will decrease more than the homogeneity. This same effect happens in figure 5D where the decrease in energy is again bigger than the one in homogeneity because is produced by directional changes in the pattern of pixel clusters.
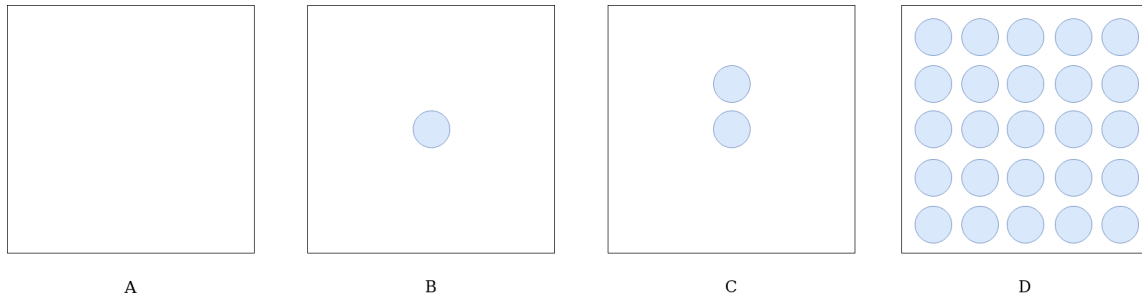
Figure 5: Images to describe how the textural parameters behave. The more circles the images include the bigger the entropy, oppositely the energy and homogeneity decrease. The energy takes into account directions, so if the circles are placed regularly it decreases faster than the homogeneity.

Image	Homogeneity	Textural Entropy	Energy
A	1	0	1
B	0.99	0.17	0.95
C	0.98	0.26	0.92
D	0.94	1.59	0.44

Table 1: Numerical results of the textural parameters computed for figure 5. The difference between energy and homogeneity becomes more clear in the values of the last image.

4.2 VOLUMETRIC PARAMETERS

Volumetric parameters are related to the shape of the colony and describe the morphology of it. So, to compute them we need images where the cell colony is clearly differentiated from the void. This is done by image segmentation, specifically by thresholding, where all the pixels below a chosen value become zero (void) and all the pixels above the threshold become one (biomass). In this project we worked with three volumetric parameters: Averages run lengths (in X,Y and Z), aspect ratio and fractal dimension.

4.2.1 *Average run length*

The average run length can be computed for each direction and it is defined as the average number of cell pixels found consecutively in the image. It can be found by dividing the total number of pixels over the total number of runs. In our system it will give an insight of the dimension of the colony.

4.2.2 *Aspect ratio*

The aspect ratio in three dimensions is defined as the relation between the average run lengths in the X (AXRL) and the Y (AYRL) direction. In this project if the measured aspect ratio is around one the colony is symmetric in X and Y. When the quantification of colonies is performed the X and Y directions are defined randomly, therefore the aspect ratio is computed placing the higher average run length on the numerator. Hence, all the aspect ratios will be bigger than one.

$$\text{if AXRL} > \text{AYRL} \rightarrow AR = \frac{AXRL}{AYRL}; \quad \text{if AYRL} > \text{AXRL} \rightarrow AR = \frac{AYRL}{AXRL} \tag{10}$$

4.2.3 *Fractal dimension*

In fractal geometry, a fractal dimension is a ratio providing a statistical index of complexity comparing how detail in a pattern changes with the scale at which it is measured [28]. In our system the fractal dimension will measure the roughness of the colony boundaries. Since we work in a three dimensional system its value should vary from one to three, the closer we got to three the more irregular the colony surface is.
There are many ways to compute it but we will use box-counting method, also known as the Minkowski-Bouligand dimension [29]. This determines the fractal dimension of a set S in a Euclidean space R^n by lying the object on an evenly spaced grid and counting how many boxes are required to cover the set. The dimension is obtained by seeing how this number of boxes changes as the grid becomes finer:

$$dim_{box}(S) = \lim_{\epsilon \to 0} \frac{\log N(\epsilon)}{\log(1/\epsilon)} \tag{11}$$

Where $N(\epsilon)$ is the number of boxes of side length ϵ required to cover the set.

4.3 STATISTICAL ANALYSIS

A correct statistical analysis allows to compare differences between parameters quantified from colonies belonging to different strains.
Having a certain data set of N elements there are several ways of defining a typical value from it, but the best estimator is the mean, $\hat{\mu}$.

$$\hat{\mu} = \frac{1}{N} \sum_i x_i = \bar{x} \tag{12}$$

The uncertainty of the mean, $\hat{\sigma}_\mu$, can be computed as:

$$\hat{\sigma}_\mu = \frac{\hat{\sigma}}{\sqrt{N}}; \qquad \hat{\sigma} = \sqrt{\frac{1}{N-1} \sum_i (x_1 - \mu)^2} \tag{13}$$

Where $\hat{\sigma}$ is the standard deviation of the data set.

If two data sets want to be compared a Student T-test can be used to analyze differences among means [30]. A T-test allows us to compare the average values of the two data sets and determine if they came from the same population. This technique can be applied if the data collected comes from independent observations, each sample should belong to only one group, there are not significant outliers in the data sets and the data for each group is approximately normally distributed. To perform a T-test three numerical values from each data set are needed:

- The mean of each data set, μ_1 and μ_2.

- The standard deviation of each population, σ_1 and σ_2 .

- The number of samples of each group, n_1 and n_2.

If the groups that want to be compared have a different number of total samples the T_{val} is computed as:

$$T_{val} = \frac{\mu_1 - \mu_2}{\sqrt{\frac{\sigma_1^2}{n_1} + \frac{\sigma_2^2}{n_2}}} \tag{14}$$

The previous expression it is also known as Welch's t-test [31]. The null hypothesis is that all populations means are exactly equal, when the null hypothesis is true T_{val} is exactly zero. Higher values of T_{val} indicate that a large difference exists between the two sample sets.

Even though the T_{val} gives an idea whether the data sets are equal, to determine if these are statistically different needs to be accompanied with the number of degrees of freedom D_{freed}:

$$D_{freed} = \frac{\left(\frac{\sigma_1^2}{n_1} + \frac{\sigma_2^2}{n_2}\right)^2}{\frac{\left(\frac{\sigma_1^2}{n_1}\right)^2}{n_1 - 1} + \frac{\left(\frac{\sigma_2^2}{n_2}\right)^2}{n_2 - 1}} \tag{15}$$

The number of degrees of freedom gives the specific T-distribution followed, in our case a two tailed distribution, and allows to compute a p_{val}. The p_{val} represents the probability of observation under the null hypothesis, and can be compared to a common significance level, α. In this study the significance is set to $\alpha = 0.05$. If the p_{val} is smaller than α it can be said that the distributions are statistically different and the null hypothesis is false.

EXPERIMENTAL STUDY

5.1 BACTERIAL STRAINS

The bacterial strains utilized in this project are mutants of MG1655, known as the strain chosen for the first published sequence of a wild-type laboratory strain of *E.coli K-12* [32]. MG1655 has been maintained as a laboratory strain with minimal genetic manipulation.

A total of five strains, listed in table 2 were studied in this thesis. Four of them are strains with specific deletions in genes encoding various bacterial surface structures that are important, among other things, for bacterial motility and adhesion processes [33].

	Name, Relevant Characteristics	Reference
MS613	MG1655 K-12 reference (F-lambda- ilvG- rfb-50 rph-1) strain	[19]
MS428	MG1655 Δfim	[34]
MS427	MG1655 Δflu	[35]
MS528	MG1655 ΔfluΔfim	[34]
NM109	MG1655fliC::kan	appendix B

Table 2: List of the strains used in the thesis. All of them are mutants of *E.coli K-12*. The table includes their relevant characteristics and reference.

Since MG1655, MS613, is the least genetic manipulated strain available from now on we refer to it as wild type or WT.

MG1655Δflu, MS427, is a strain which carries a deletion in the gene encoding the auto-transporter protein antigen 43. Antigen 43 is a handshake protein that confers characteristic surface properties such as autoaggregation and a frizzy colony morphology [36]. It is important for cell–cell aggregation and cellular chain formation. Large amounts of this protein are expressed, approximately 50,000 copies per cell, in the outer membrane of various bacterial species including *E. coli*.

The MG1655Δfim, MS428, strain does not express pili, also known as type I fimbriae. Pili are filamentous adhesive organelles of $1-2$ μm long found in the surface of bacteria [37]. They are important for cell-surface and cell-cell adhesion. Its expression is essential for the pathogenicity of gram-negative bacteria. A double mutant MG1655 Δ fluΔ fim, MS528, that does not express pili nor antigen 43 was also available.

Lastly the strain MG1655fliC::kan, NM109, is presented. This strain does not express flagella.

Bacterial flagella are helically shaped structures containing the protein flagellin that are involved in numerous locomotion processes [38] briefly introduced in chapter 2.

(a) Structures deleted in the different strains

(b) *E.coli* transmission electron microscopy image
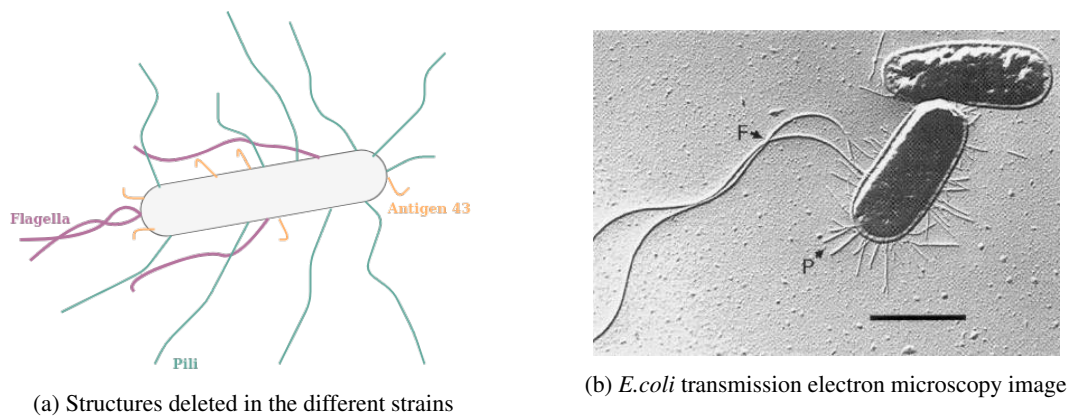
Figure 6: (a) Representation of the structures suppressed in the cell strains used in the project. Antigen-43, with an exaggerated shape and size, are sketched in yellow and pili in turquoise. Flagella are drawn in purple and are responsible of many of the motility processes bacteria can perform. (b) Transmission electron microscopy images of *E.coli*. Pili, marked with a P, and flagella, marked with an F can be observed. Antigen-43 is too small to be visualized in the scale that corresponds to 1 μm. Image from [39].

All the different structures can be visualized in figure 6, these are thought to be critical in the early stages of biofilm formation. So, looking at differences between colony morphologies for the different strains plenty of information can be gained. For example, discrepancies between Δflu and Δfim colonies could indicate that autoaggregation mediated by antigen-43 is somehow blocked by fimbriation as is suggested in some studies [40].

All the strains were kept frozen without a fluorescence plasmid, but some of them were also available as two different labeled strains containing a fluorescence plasmid, pVS130 expressing cyan fluorescent protein or pVS132 expressing yellow fluorescent protein [41]. This plasmids were previously introduced in WT, Δflu,Δfim and ΔfluΔfim strains by a transformation process. In the case of the non-flagellated strain ΔfliC a chemical transformation, which protocol is described in appendix C, was performed during this study to generate two new strains containing each of the fluorescent plasmids that the other strains already incorporated.

5.2 MOTILITY ASSAY

A swimming assay gives information about the ability of a particular bacterial strain to move in a semisolid media. The migration in this assay is aided by chemotaxis as bacteria move to regions with higher nutrient levels.

To perform the assay 1 μl of overnight culture is inoculated in the center of a Petri dish that contains media with a particular agar concentration. The whole protocol can be seen in appendix D. Swimming is usually tested in plates containing a 0.3%(w/v) of agar or even smaller. Since the aim of this thesis is to study colonies in semi-solid media it is more interesting to observe the motility of the strains in concentrations bigger or equal than 0.3%. So, in this assay higher agar concentrations are used and is

more appropriate to call the experiment a motility assay rather than a swimming assay.

To know if the motility was influenced by several types of environmental stress, apart from a different agar concentration, the motility was tested in plates with changes in the nutritional properties of the media.

Therefore, the final assay was performed for three different media: Lysogeny broth (LB), M63 minimal media (MM) and M63 minimal media supplemented with casamino acids (MMCA) for Petri dishes with five possibles agar concentrations 0.3%, 0.4%, 0.5%, 0.6% and 0.7%. How the different media and plates were prepared is explained in appendix A. At the end, every strain was tested under a total of fifteen different conditions.

5.3 COLONY FORMATION

The principal experiment of this project is the growth of three dimensional bacterial colonies in semi-solid agar. The main idea is to place isolated bacteria in a thin layer of semi-solid media where they can grow in a three-dimensional space.

The experiment starts with an overnight culture of a desired bacterial strain. In an overnight culture a single colony from a solid plate is placed in 3 ml of LB media supplemented with antibiotics, and put in the incubator at 37ºC for 8 h with shacking. Since the number of cells in the colonies used for the overnight changes every time, a good way to known the final number of cells in the solution is measure its optical density (OD600) with an spectrophotometer. A description of how this is done can be found in appendix F. From this value the number of cells in the solution can be easily estimated and in general for saturated cultures it is around 10^9 cells/ml.

Knowing the OD600 value of the overnight culture, this culture can be repeatedly diluted until obtaining a solution of around 1 $cell/\mu m$. It usually takes 3 dilutions, in each of those $10\mu l$ of the previous solution is placed in 1 ml of fresh LB media as can be seen in figure 7.

When the desired concentration is obtained 10 μl of this are placed in an Eppendorf tube containing 1 ml of a certain media with a certain agar concentration supplemented with antibiotics that until that point has been placed in a block heater at 55 $°C$ where the agar is in liquid state. For the particular plasmids that the strains in this project include, pVS132 and pVS130, the Eppendorf tube should contain ampicillin and additionally IPTG. IPTG is a molecular biology reagent that in this system chemically induces the expression of the plasmids [42].

Once the bacteria are mixed with the agar the whole content of the tube should be poured quickly into a glass bottomed Petri dish. When the agar solidifies the dish is placed in the incubator for as long as wanted. The complete protocol for this experiment is described in appendix E.

Following this protocol the final thickness of the agar layer in the Petri dish is around 300 μm. This value is appropriated as we want to avoid a really thick agar layers where differences in the colonies can arise as a consequence of the depth in the layer where they grow. So, after a certain incubation time the observable colonies should present a diameter around 300 μm. If colonies are bigger than that will indicate that they have reached the top of the plates and their growth is not three dimensional anymore.

The experiments were performed so the final agar concentration in the plates was 0.5%. About the nutritional media of the plates, three different media were available and tested to decide which one was more convenient:

- Lysogeny broth, colonies reached the appropriate size after 12h of incubation.

- M63 Minimal Media, colonies reached an appropriate size after 15h of incubation.

- M63 Minimal Media supplemented with casamino acids, colonies reached the appropriate size after 14h of incubation.

Comparing the incubation time and the performance under a confocal microscope, is to say the level of background noise of each media, M63 minimal media was the one chosen to perform the experiments.
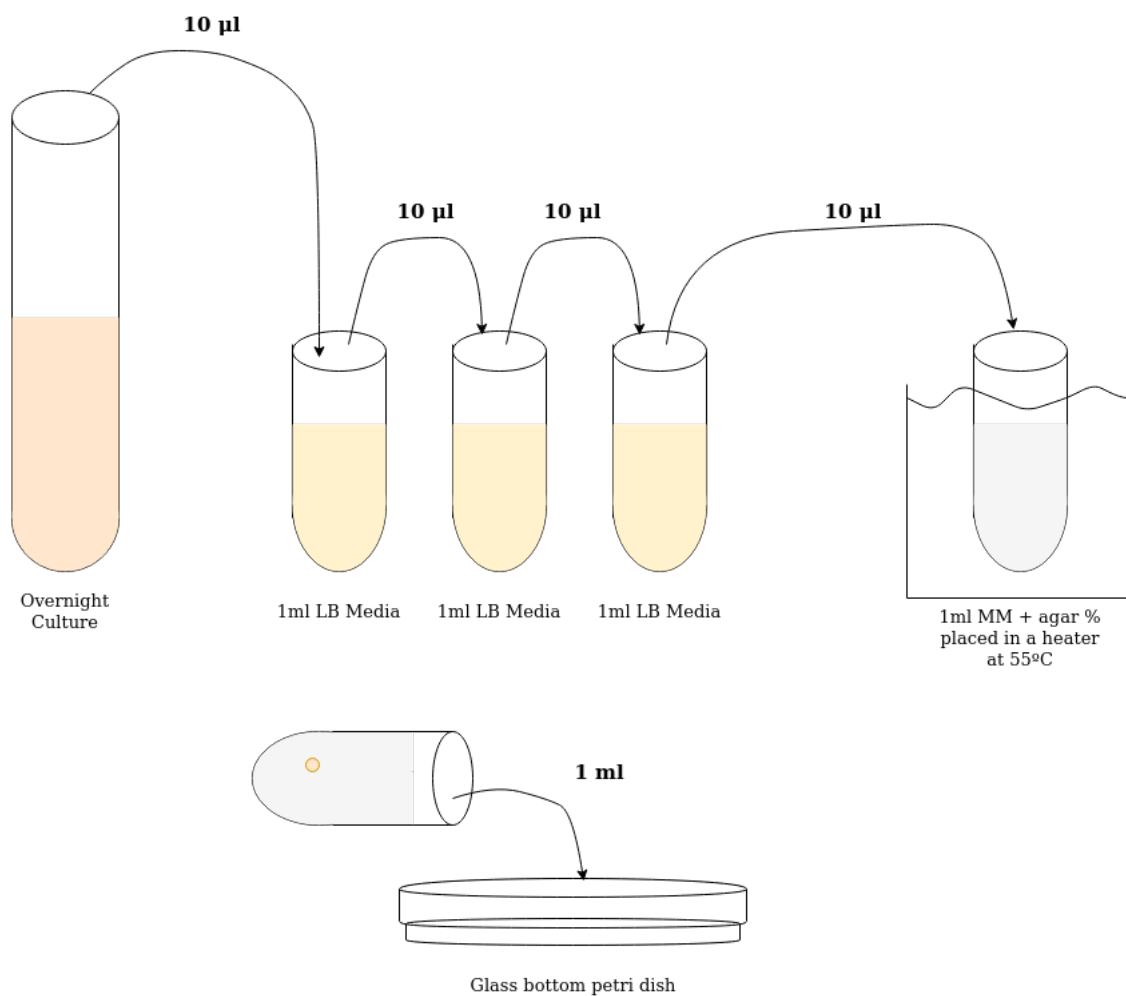
Figure 7: The figure shows the main steps that need to be followed to grow three dimensional bacterial colonies. In particular shows how the serial dilution is usually performed, from the first dilution of the saturated overnight culture, once its OD600 value is known, to the one where the diluted content is mixed with the agar placed in the heater and the later pouring of its content in a glass bottomed Petri dish.

5.3.1   *Effect of Agar concentration*

With the experimental setup described in the previous section, a simple change in the agar concentration of the media where the colonies grow will allow us to study a phenomenon observed in other investigations. Mitchell and Wimpenny [43] studied multiple bacterial species growing at different agar concentrations. They grew subsurface colonies and observed motile species producing large colonies at low agar concentrations that changed its behaviour above a critical value between 0.5% and 0.6% (w/v) agar. The bacteria produced then small lenticular colonies independent of an increase to even higher concentrations.

The mechanisms behind agar concentration changing the colony morphology have not been determined yet, but it seems that the greater the concentration the more elongated the colonies are expected to be. To test this result, the growth of three dimensional colonies was performed in two additional semi-solid medias:

- Petri dishes with lower agar concentration, 0.4%(w/v).

- Plates with higher agar concentration, 0.6 %(w/v).

5.3.2   *Image processing*

The colonies were imaged with a LEICA SP5 confocal microscope. In the setup at our disposal the microscope had eight different excitation wavelengths: 405, 458, 476, 488, 496, 514, 543 and 633 nm. As presented in section 5.1 each strain was available containing two different plasmids: pVS130 eCFP and pVS132 YFP. The spectra of these fluorophores can be seen in image 8. Comparing the spectra and the usable wavelengths we can see how the required excitation wavelength for the YFP fluorophore is available in the setup. Therefore, it was clear that the study should be developed with the mutants containing the YFP plasmid. Hence, colonies were imaged with the laser of wavelength 514 *nm* and a detection length typically placed between 525 and 580 nm.
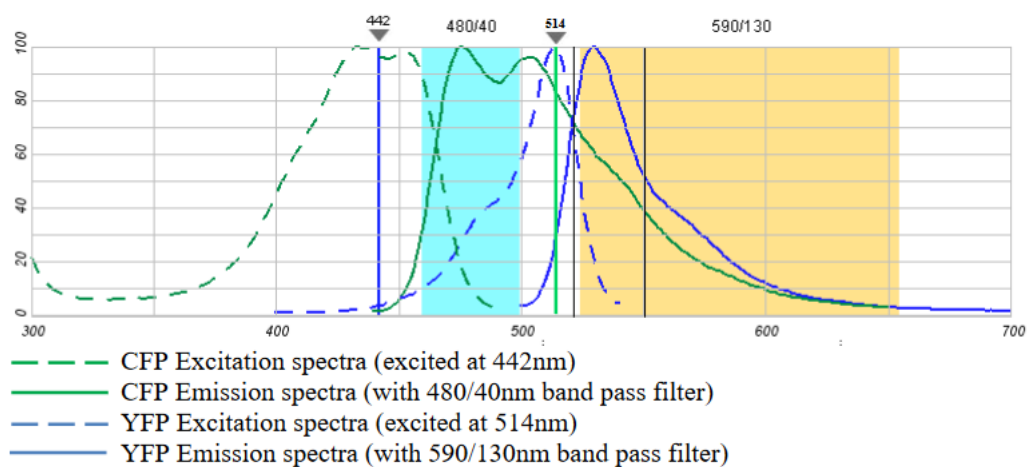
Figure 8: Plasmid Spectra of YFP and CFP, from Invitrogen's spectra viewer [44]. Comparing the maximum of the excitation spectra with the available excitation wavelengths it seems more reasonable to work with mutants including YFP.

An air objective $NplanL20x0.40corr\infty/0-2/C506057$ was chosen to visualize the colonies, since objectives with higher magnification had really small apertures and the signal intensity emitted by the cells was not good enough to image them with greater precision.

Once the confocal microscope generated the stacks some image processing was needed before proceeding to quantify the colonies following the guidelines given in chapter 4. FIJI (Fiji Is Just ImageJ) [45] was the software chosen for that. The image processing workflow followed in this project can be summarized as:

1. Remove initial and final stacks of the imaged colonies.

2. Apply background noise reduction. Required for some of the colonies. It was done by adjusting the Brightness/Contrast since the background was relatively even across the images.

3. Compute textural parameters following section 4.1 definitions. This is done with a custom python script.

4. Apply threshold to distinguish the colony from the void. Threshold following the Otsu method [46]: binarization algorithm that involves iterating through all the possible threshold values and calculating a measure of spread for the pixel levels each side of the threshold.

5. Perform a 3D binary interpolation, included in the 3D ImageJ Suite plugin [47].

6. If the colony is partially hollowed:

    • Find boundary of the colony with: *Find Edges*. Process included in the FIJI processing menu. It uses a Sobel edge detector to highlight sharp changes in intensity in the image [48].

    • Close the edges of the colony with: *Binary -Close*. It is included in the FIJI binary submenu and performs a dilation operation, followed by erosion [48].

    • Fill the closed colony sections with: *Binary -Fill holes*. It is included in the FIJI binary submenu, and fills holes, defined as four connected background elements, in binary objects [48].

   Repeat previous steps until a completely filled colony is obtained.

7. Compute Volumetrical parameters following section 4.2 definitions. This is done with a custom python script. To compute the fractal dimension just the colony surface is required so the filled colony has to be processed with *Find edges* one last time.

Figure 9: Figure to illustrate different steps of image processing for the same slice of a colony. In figure A the colony after subtracting the background noise can be seen. In figure B a threshold has been applied and step six has been performed until obtaining a filled colony. In figure C the edges of the colony are found to compute its fractal dimension.

In figure 9 the same slice of an experimental colony is shown at different points of the image processing steps. Figure 10 shows a three dimensional reconstruction of the colony where the cross section comes from for the same steps as figure 9. This reconstruction is done with 3D Viewer FIJI plugin [49].
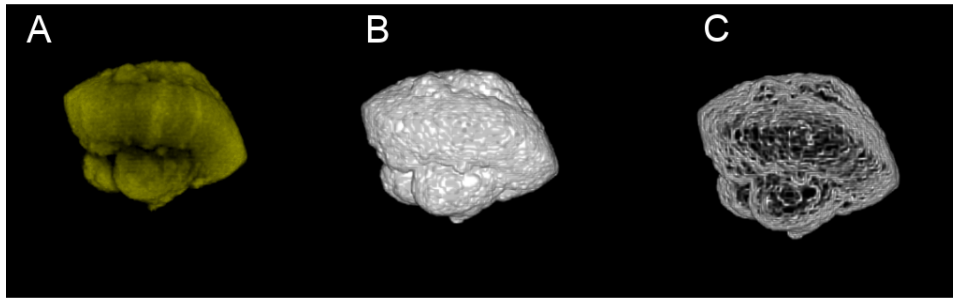
Figure 10: Three-dimensional reconstruction of the colony shown in figure 9 for each of the described processing steps in that figure.

In the first processing step it is said that final and initial colony stacks have to be removed. This can be explained looking at how the experimental colonies are imaged. The stacks are obtained once two Z-positions are defined. The first Z-position is defined when the colony is not visible yet, and the last one is chosen once the colony shape has completely faded. But the colony fading in this last slice does not implies that it ends there. When using confocal microscopy the excitation light has to penetrate the sample as the focal point moves deeper into the colony, meaning that the material between these will absorb an scatter some of the emission and excitation light. So, when we image a colony we are only able to gain information about its bottom half. This half starts fading as we reach a certain depth in the sample, and since we are working in three dimensions the spatial configuration of the colonies can change so the depth when the fading starts varies between different sections of a same colony. Therefore, for each colony a cutoff in the Z stacks needs to be done. This cutoff is done when some section of the colony starts fading. A colony before and after this cutoff can be seen in figure 11.

Figure 11: Figure showing the same colony before (A) and after a cutoff (B) in the Z stacks. The images show the maximum intensity X-projection of the colony.

EXPERIMENTAL RESULTS

In this chapter the most relevant results obtained from the experimental methods are presented and discussed.

6.1 MOTILITY ASSAY

The motility assay results were obtained after incubating the plates for 24 h at 37ºC. The plots show the biggest diameter the cells achieved from its inoculation point. The Petri dish used in the assay had a diameter of 96 mm and in some conditions the bacteria reached the edge of this, therefore, the maximum dish diameter is included in the figures as it acted as a limit in the spreading. The plots do not include error bars since each point correspond to a single measure. For the discussion of results we consider 0.3%-0.4% as low agar concentrations, 0.5% as medium agar concentration and 0.6%-0.7% as high agar concentrations.

Even though the plots show the values after 24 h hours of incubation the plates with M63 minimal media as nutritional source were left 24 additional hours in the incubator to discard a low motility as a consequence of a smaller doubling time. The results obtained after that time were not significantly different.
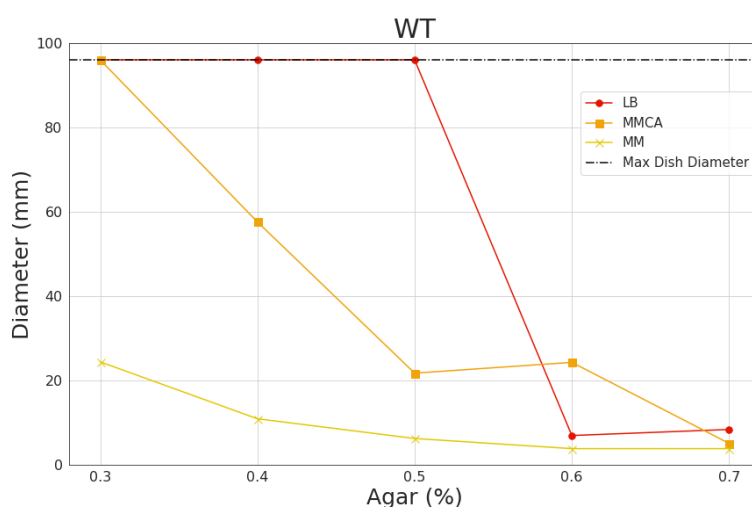
Figure 12: Motility assay results of the wild type (WT), MG1655 strain. The maximum diameter value versus the agar concentration is plotted for each media: M63 minimal media (MM), Lysogeny broth (LB) and M63 minimal media supplemented with casamino acids (MMCA). A different behaviour between the three media can be observed, this becomes more clear as the agar concentration decreases.

In figure 12 the results of the assay for the wild type strain (WT) are plotted. Looking at them, it is clear that a dependence exists between the nutritional level of the media and the efficiency of the cell movement. In low agar concentrations cells are able to move no matter the media, however, the higher the nutritional level the bigger is the maximum distance achieved. In medium agar concentration the movement in MM is significantly reduced, while LB and MMCA do not experience such a big change. For higher agar concentrations, as the cells stop moving, the difference between mediums becomes negligible.

(a) Motility assay Δflu strain

(b) Motility assay Δfim strain
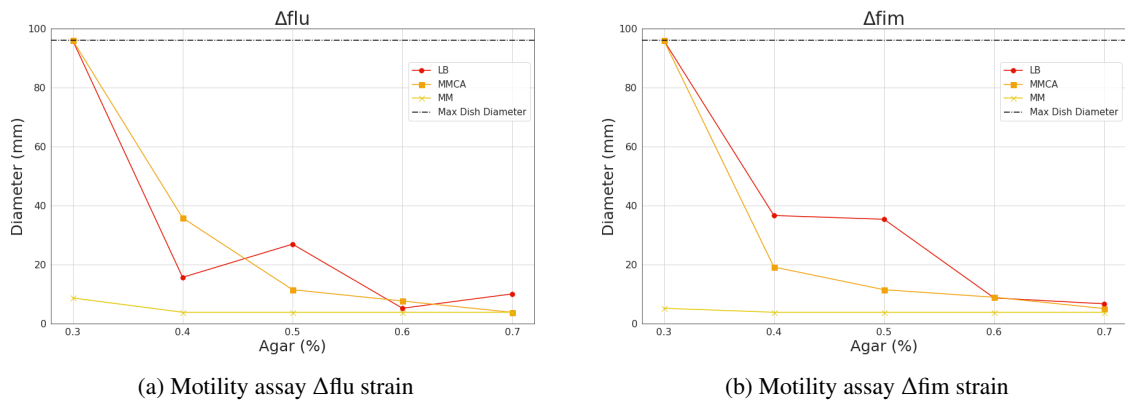
Figure 13: (a) Motility assay results of the strain with a deletion in the gene encoding antigen 43, Δflu. (b) Motility assay results of Δfim which does not express pili. In both figures the maximum diameter value versus the agar concentration is plotted for the three media. The maximum diameter achieved, for all media, is reduced as the agar concentration increases.

(a) Motility assay ΔfluΔfim strain

(b) Motility assay ΔfliC strain
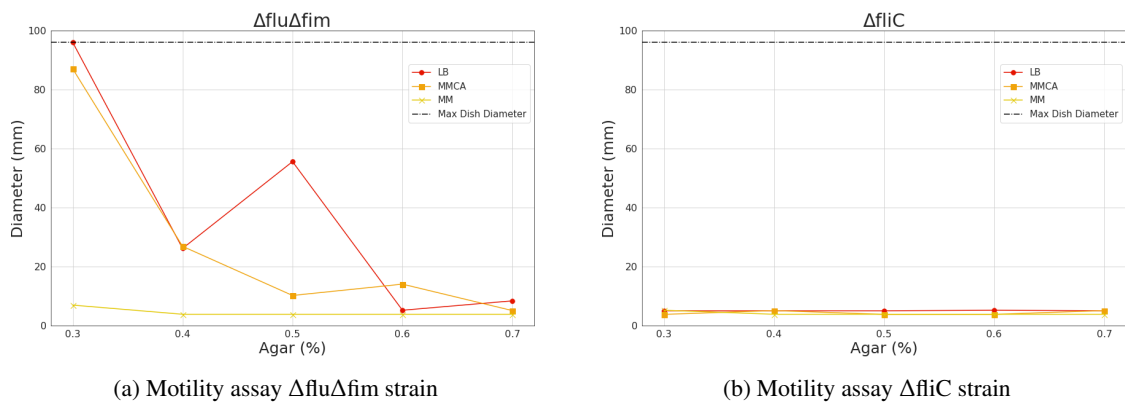
Figure 14: (a) Motility assay results of ΔfluΔfim, the double mutant that does not express pili nor antigen 43. The maximum diameter value versus the agar concentration is plotted for the three media. The maximum diameter achieved, for all media, is reduced as the agar concentration increases. (b) Motility assay results of ΔfliC strain which does not express flagella. The maximum diameter value versus the agar concentration is plotted for the three media. No bacterial movement was noticed in the experimental plates no matter the media or agar concentration.

Figure 13(a) shows the results of the assay for Δflu strain, the mutant with a deletion in the gene encoding antigen 43. Figure 13(b) plots the points obtained for Δfim strain, the mutant without pili and figure 14(a) the double mutant results ΔfluΔfim. The three strains behave similarly under the same conditions. A dependence with the nutritional media is also observed at low agar concentrations, but as the concentration increases the motility is equally reduced. In MM cell motility is just perceivable at 0.3% agar. For MMCA and LB media the overall motility of these strains seems to be reduced if it

is compared to the results obtained under the same conditions for the WT strain. This means that even all the mutants present flagella their expression is not sufficient to achieve the same motility efficiency as the wild type cells.

In figure 14(b) the experimental results of the ∆fliC strain, the non-flagellated mutant, are plotted. In this strain there was no perceptible motility no matter the media or agar concentration, this motivates the conclusion that flagella are the principal responsible of bacterial motility in this experiment. However, as seen in the rest of the mutants having only flagella does not mean that the cells will be able to achieve the most efficient mechanism of motility. To explain why this happens two hypothesis are proposed. In the first one it can be said that there are other structures apart form the flagella important for bacterial motility, in the second one the reduction of motility in the mutants can be seen as if an over-expression of other structures block the normal production of flagella [50].

In general, seems that the higher the nutritional level of the media the further the cells can move under a same agar concentration. This can be for metabolic reasons but it is also possible that the different media components affect the stiffness of the plate, as seen in some studies [51] where salines and richer media present a shift in its elastic moduli value when prepared for the same agarose concentration. So, even though the plates of different media were made with the same agar concentration to provide an equal stiffness fluctuations in the real value of it can be found.

Since the media chosen to grow the three-dimensional colonies is M63 minimal media, it is worth it to compare the motility of the strains on it. In figure 15 the motility assay for all the strains in MM are plotted. The only agar concentration were all the strains are able to move is 0.3%, even though the WT strain moves much more than the rest. Comparing the mutants, at 0.3%, we see that the non-flagellated strain is the one that moves the less, followed by the strains with pili deletion. For concentrations higher than 0.3% the only strain that is able to move is the WT.
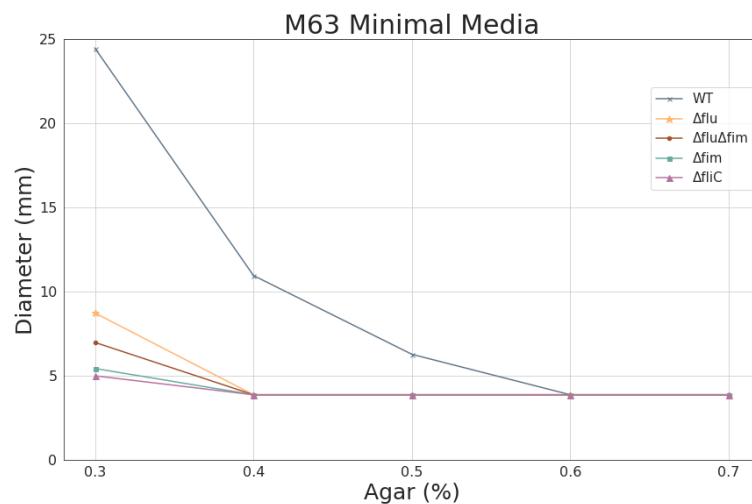
Figure 15: Motility assay for all the strains in M63 minimal media. The maximum diameter achieved versus the agar concentration is plotted for each strain. The maximum diameter is reduced as the agar concentration increases for all the strains.

In the main experiment of this project colonies were grown in 0.5%(w/v) agar, in this value the only strain with motility observable in a macroscale is the WT. However, the maximum distance achieved by it is not big enough to compromise the formation of colonies. The formation of colonies could also tell if some of the other strains are motile in a microscale.

6.2 COLONIES IN 0.5% AGAR CONCENTRATION

In this section, the colonies grown in M63 minimal media with an agar concentration of 0.5% are presented and quantified. The five strains were imaged after an incubation time of 15 h. The study concluded with 39 samples of the wild type strain (WT), 21 of the mutant with a deletion in the gene encoding antigen 43 (Δflu), 17 of the strain that does not express pili (Δfim), 15 of the double mutant (Δflu Δfim) and 23 of the non-flaggelated cells (ΔfliC). The full data set can be found on [52].
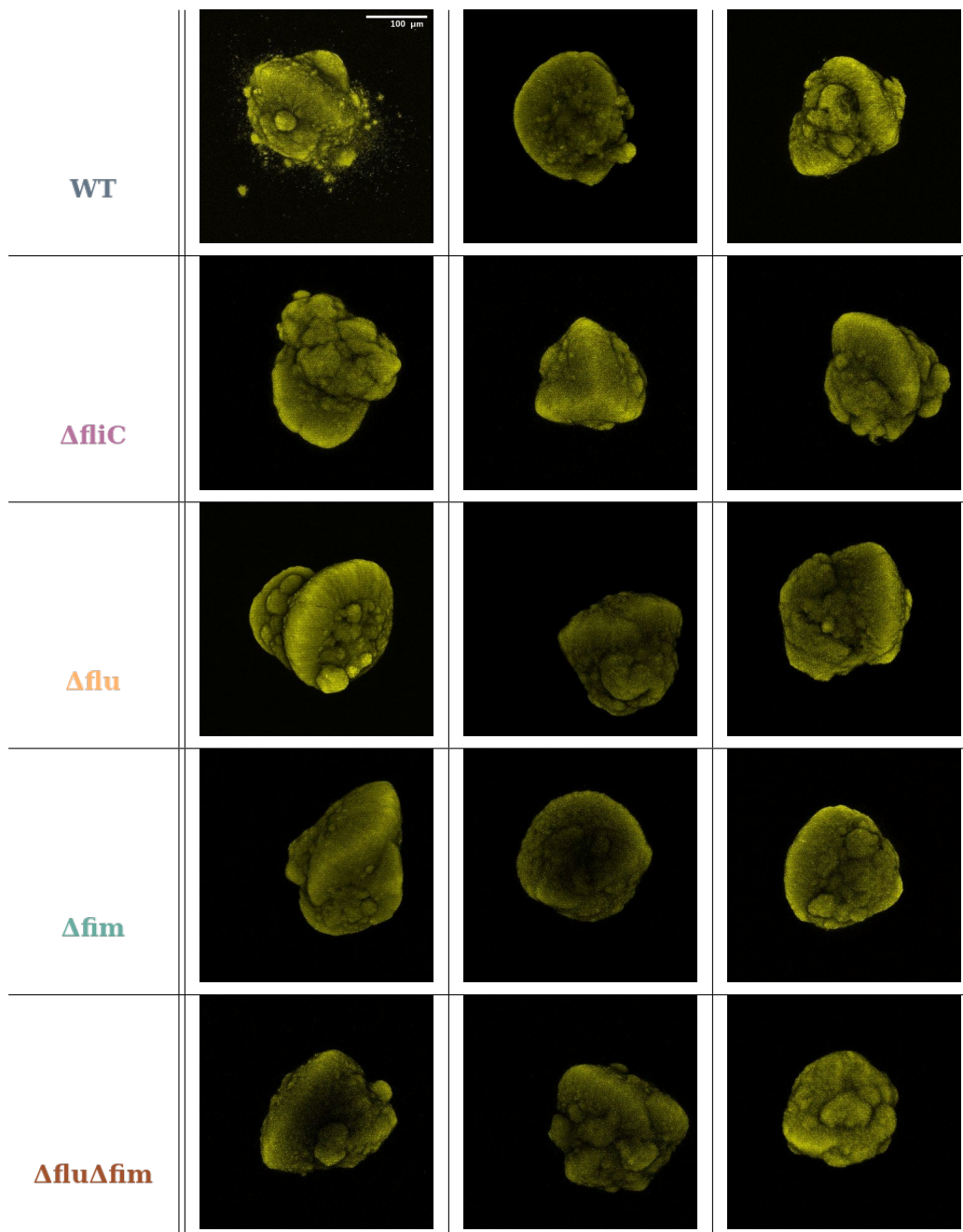
Table 3: Colonies at 0.5% Agar concentration. The table shows maximum intensity Z-projections of colonies imaged after 15 h of incubation time. There are three colonies per strain and the scale is the same for all images.

Table 3 contains some of the colonies obtained experimentally, they have been chosen to show as many morphologies as possible. Some of them look quite spherical, for example in the second column of Δfim, but its surface seems far from being uniform, as can be seen in the third column of the ΔfluΔfim strain. Nevertheless, the vast majority of observed colonies deviates from a round shape. They often present protuberances or a more elongated shape, as may be seen in the first column of Δfim. The more elongated morphologies tended to appear more frequently in some of the experimental plates than in others.

Aside from the overall morphology of the colonies an interesting phenomena was also observed, this is discernible in the first column of the WT strain. Some of the colonies presented small fluorescent aggregates, from now on called satellites, around them. Table 4 contains more colonies that presented satellites, these were just observed in the WT strain.
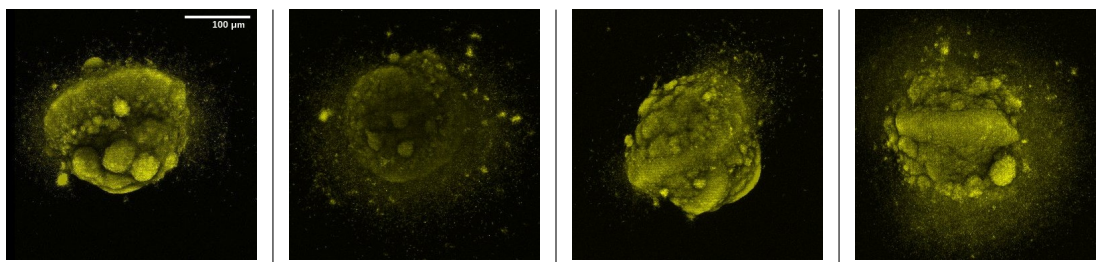
Table 4: Maximum intensity Z-projections of colonies that present satellites after 15 h incubation time in MM and 0.5% agar. All the images correspond to the WT strain.

Knowing the differences between the motility of WT and the mutants in M63 minimal media and 0.5% agar concentration, lead us to think that the emergence of satellites is a direct consequence of bacterial motility. Its formation can be thought as if they appear when some bacteria, presumably in the colony surface, are able to detach themselves from the aggregate and move on its surroundings until they stop and start growing as another aggregate. This satellites can be observed as compact aggregates of around 10 μm and the colonies where they appear are typically accompanied by a noisy signal around its surface. In the whole data set of WT just 9 colonies presented this anomaly and they appeared in Petri dishes where colonies without satellites were also growing.

Except for the colonies that present satellites, looking at the images it is difficult to tell if a colony belongs to one strain or another. A colony quantification is required to try to find some differences between strains. The colonies were quantified following the steps described in section 5.3.2. The distributions of the different parameters for the strains can be seen in appendix G. Once a parameter is computed for all the samples of one strain a T-test can be performed to compare this results with the other strains. The T-test will tell if the populations are statistically different and its results are analyzed under a significance of $\alpha = 5\%$ ($p_{val} = 0.05$).

The distributions of the different parameters can be seen as box plots. This representation is chosen because it is a standardized way of displaying distributions of data, and the spread out of its values, with a five number summary:

- Maximum, the largest data point excluding outliers, seen at the end of the top whisker.

- Minimum, the lowest data point excluding outliers, seen at the end of the bottom whisker.

- Media, the middle value of the dataset, represented as a notch.

- First quartile, median of the lower half of the dataset, seen at the bottom of the box.

- Third quartile, median of the upper half of the dataset, seen at the top of the box.

The box plot shape will show if a statistical data set is normally distributed. If the median is in the middle of the box and the whiskers are about the same on both sides of the box, then the distribution is normal. If the median is closer to the bottom of the box the distribution is positively skewed. Otherwise, the distribution is negatively skewed. The outlier points are represented as white circles and the plots also include the mean of the distribution, represented as a black dot.

Energy

The box plot of the energy at 0.5% agar concentration for the different strains is shown in figure 17. Smaller values of textural energy correspond to more frequent patterns of pixels clusters, the strain with the smallest mean energy is Δflu, whereas the strain with biggest mean energy is ΔfliC.
The results of the statistical test to compare the results can be seen in table 5. Looking at the p_{val} it is clear that WT is significantly different of Δflu and ΔfliC, and that these two are also significantly different between them. The strains that present pili deletion Δfim and ΔfluΔfim are not statistically significant of any strains, this can be explained by looking at their distributions in figure 44 and figure 45 in appendix G. One of the conditions to perform a T-test is that the variables should be normally distributed and the distributions of these strains look more uniform. If these strains are actually not different from the rest could be known by increasing the number of experimental points and obtaining a more normal distribution.

Entropy

Figure 20 shows the box plot of the entropy at 0.5%(w/v) agar for the different strains. Bigger values of textural entropy correspond to more heterogeneous images, the strain with the biggest entropy mean value is Δflu, whereas the strain with smallest mean value of entropy is ΔfliC.
Looking at the p_{val}, in table 5, it is clear that WT is significantly different of Δflu and ΔfliC, and that these two are also significantly different between them. The double mutant, ΔfluΔfim is significantly different of ΔfliC but not from any other strain, and Δfim is not statistically significant of any strains. Again, this results can be explained by looking at their distributions in appendix G, figure 49 and figure 50.

Homogeneity

The textural homogeneity box plot at 0.5% agar concentration for the different strains can be seen in 23. A bigger homogeneity is related to more homogeneous images, the strain with the biggest homogeneity mean value is ΔfliC and the one with the smallest is Δflu. This results agree with the ones obtained for the textural energy, but it is important to note that the homogeneity values are bigger

than the energy ones. Homogeneity measures repeating patterns of pixels clusters and energy takes into account directional variations in the pattern of these, a disruption in the homogeneity of an image results in a faster decrease of textural energy than textural homogeneity.

Looking at table 5 WT is significantly different of Δflu and ΔfliC strain, and that these two are also different between them. The double mutant, ΔfluΔfim is different of ΔfliC but not from any other strain, and Δfim is not statistically significant of any strains. Their distributions, figure 54 and figure 55 in appendix G, are again more uniform than normal.

	Energy		Entropy		Homogeneity	
	T_{val}	p_{val}	T_{val}	p_{val}	T_{val}	p_{val}
WT / ΔfliC	-2.61	0.012	2.89	0.005	-3.35	0.0014
WT / Δflu	2.48	0.017	-2.25	0.028	1.988	0.051
WT / Δfim	-0.87	0.39	0.94	0.35	-0.94	0.35
WT / ΔfluΔfim	0.42	0.67	-0.69	0.49	0.562	0.579
ΔfliC / Δflu	4.48	6.17e-5	-5.13	7.1e-6	5.27	4.3e-6
ΔfliC / Δfim	1.12	0.27	-1.33	0.192	1.39	0.175
ΔfliC / ΔfluΔfim	1.90	0.070	-2.45	0.0229	2.633	0.015
Δflu / Δfim	-2.47	0.020	2.65	0.013	-2.27	0.031
Δflu / ΔfluΔfim	-0.84	0.41	0.60	0.55	-0.61	0.545
Δfim / ΔfluΔfim	0.93	0.35	-1.27	0.21	1.174	0.249

Table 5: Table showing the T_{val} and p_{val} of the quantified textural parameters for the colonies growing at 0.5% agar concentration. This results are analyzed under a significance of $\alpha = 5\%$.

Aspect Ratio

Figure 26 contains the box plot for the aspect ratios of the different strains at 0.5%(w/v) of agar. By how it is defined in chapter 4 the aspect ratio is never smaller than one, meaning that the closer it is to one the more spherical a colony is. The bigger the aspect ratio the more asymmetrical or elongated is the shape of the colony. The strain with bigger mean aspect ratio is Δflu and the strain with smaller aspect ratio is ΔfliC.

By looking at the p_{val} in table 6 the only distinguishable strains are ΔfliC with WT and Δflu. In general the T-test of the aspect ratio tells us that the populations are equal over the strains. This matches with the observed colonies, where the same variations in colony morphology are observed no matter the strain.

Fractal Dimension

The box plot for the fractal dimension at 0.5% agar concentration can be seen in figure 29. Since we study three dimensional objects, its value is expected to be between one and three. The higher the fractal dimension value the more irregular the surface of a colony is. The strain with the most irregular surface is WT, whereas the more regular surface is observed in the Δfim strain.

When performing a T-test with significance of $\alpha = 5\%$ the only strains statistically different are WT and Δfim.

As seen in the appendix G figures all the strains present similar distributions and are far from being close to three. Therefore, it begs the question on whether the fractal dimension quantification depends on the magnification used to image the colonies.

	Aspect Ratio		Fractal dimension	
	T_{val}	p_{val}	T_{val}	p_{val}
WT / ΔfliC	2.87	0.0058	0.56	0.572
WT / Δflu	-0.6227	0.53	1.57	0.124
WT / Δfim	0.86	0.39	2.481	0.018
WT / ΔfluΔfim	0.875	0.38	1.054	0.29
ΔfliC / Δflu	-2.91	0.0072	0.636	0.528
ΔfliC / Δfim	-0.844	0.409	1.22	0.23
ΔfliC / ΔfluΔfim	1.493	0.150	0.062	0.95
Δflu / Δfim	1.25	0.21	0.652	0.518
Δflu / ΔfluΔfim	1.33	0.192	-0.810	0.423
Δfim / ΔfluΔfim	-0.18	0.85	-1.672	0.106

Table 6: Table showing the T_{val} and p_{val} of the quantified volumetric parameters for the colonies growing at 0.5% agar concentration. This results are analyzed under a significance of $\alpha = 5\%$.

6.3 COLONIES IN 0.4% AGAR CONCENTRATION

In this section the colonies grown in M63 minimal media with an agar concentration of 0.4% are presented and quantified. The five strains were imaged after an incubation time of 15 h. The study concluded with 2 samples of the wild type strain (WT), 7 of the mutant that does not express antigen 43 (Δflu), 7 of the strain with a pili deletion (Δfim), 8 of the doble mutant (Δflu Δfim) and 5 of the non-flagellated strain (ΔfliC), the full data set can be found on [52].
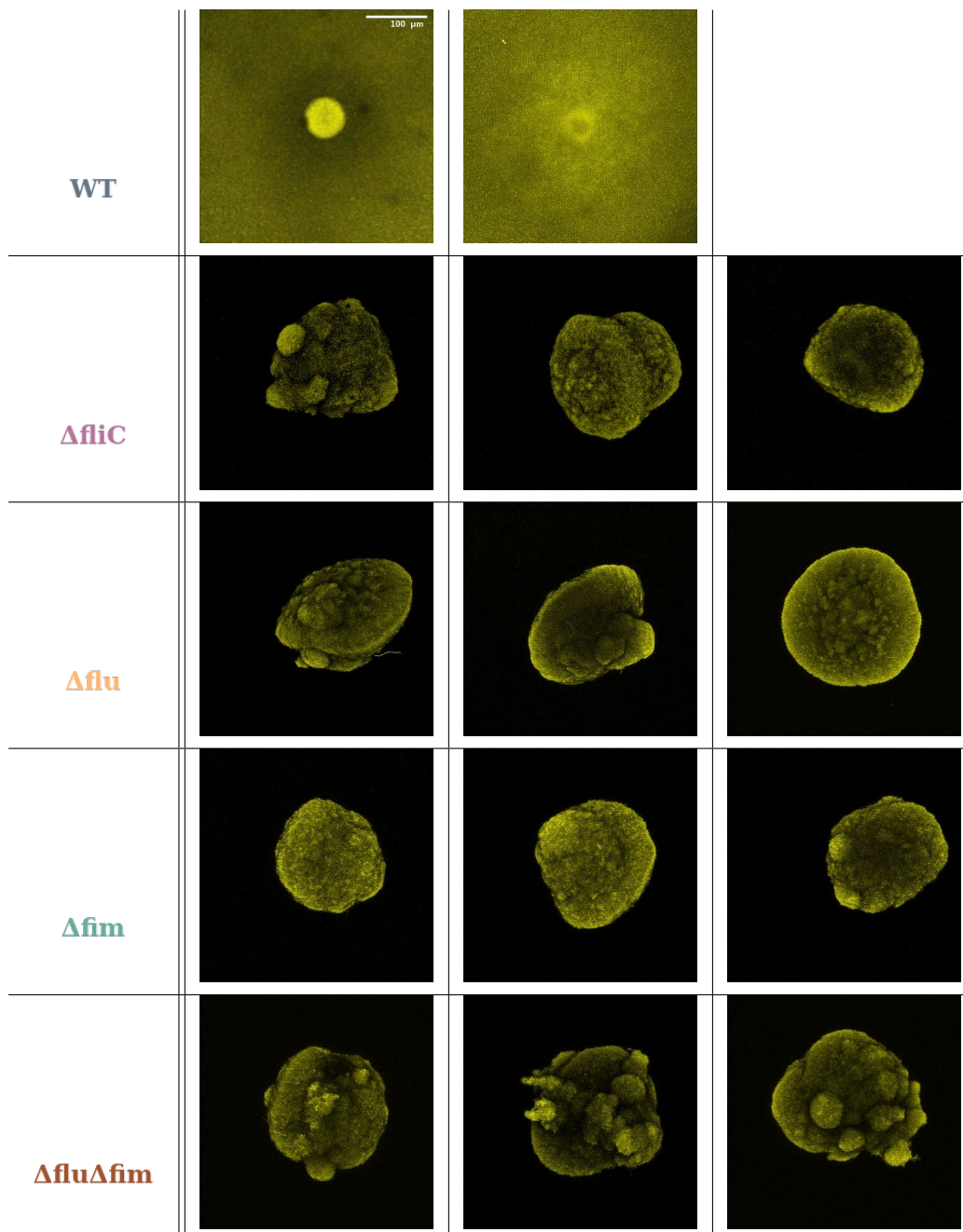
Table 7: Colonies at 0.4% Agar concentration. The table shows maximum intensity Z-projections of colonies imaged after 15 h of incubation time. There are three colonies per strain and the scale is the same for all images.

For the wild type no compact colonies were observed in this agar concentration, as can be seen in table 7. The WT bacteria spread inside the agar without forming a solid colony, this behaviour was observed by eyesight where the colonies in the plates looked much bigger than expected. For the rest of the strains there was no bacterial spreading in the media. The different behaviour can be explained by looking at figure 15 where can be seen how the WT strain increases its motility at 0.4%(w/v) regarding 0.5%(w/v) but the rest of strains remain in-motile under the change. Observing this motility supports that the satellites observed for WT could have an origin in the same phenomena. The colonies at 0.4% agar concentration presented overall a more spherical shape, this can be seen at the third column of Δflu or at the first Δfim column. However, its surface was also far from uniform in most cases.

In this concentration it is difficult too to tell if a colony belongs to one strain or another, a quantification of the colonies is required. In this case the WT colonies are excluded, since the images obtained are not comparable to the rest. Regardless the number of points in the data set being small, a T-test under a significance of $\alpha = 5\%$ is performed to have an idea of the differences between strains.

The **Energy** box plot can be seen at figure 16, the strain with biggest mean value is ΔfliC, and the smallest mean value is observed in Δfim. Figure 19 shows the **Entropy** box plot, the biggest entropy belongs to Δfim and the smallest to ΔfliC. The **Homogeneity** box plot can be found in figure 22, the strains with biggest and smallest values concur with the ones for the energy. In this concentration the values for the textural energy and the textural homogeneity are quite similar, meaning that the pixels clusters that break the homogeneity does not seem to have any directional variation. The results of the T-test for the textural parameters can be seen at table 11, from it we can conclude that the only strains that are not statistically different in a 0.4% agar concentration are Δflu and Δfim.

The **Aspect ratio** box plot, seen in figure 25, shows that the strain that deviates the most from an spherical shape is Δflu and the more spherical is ΔfliC. Figure 28 shows the **Fractal dimension** box plot, the most uniform surface is on ΔfluΔfim and the most structure is found in ΔfliC. The results of the T-test for the volumetric parameters are included in table 12, from it we can see that the comparing aspect ratios Δflu is statistically different from ΔfliC and Δfim. However, this changes when looking at the fractal dimension, where none of the strains are different from each other. This uniformity when all the other parameters in 0.4% are different between strains supports the idea that the fractal dimension value is being restrained by the objective used to image the colonies.

6.4 COLONIES IN 0.6% AGAR CONCENTRATION

In this section the colonies grown in M63 minimal media with an agar concentration of 0.6% are presented and quantified. The colonies were imaged after an incubation time of 15 h. The study concluded with 5 samples of the wild type strain (WT), 4 of the mutant with a deletion in the gene encoding antigen 43 (Δflu), 6 of the strain that does not express pili (Δfim), 5 of the double mutant (ΔfluΔfim) and 5 of the non-flagellated strain (ΔfliC). The full data set can be found on [52].
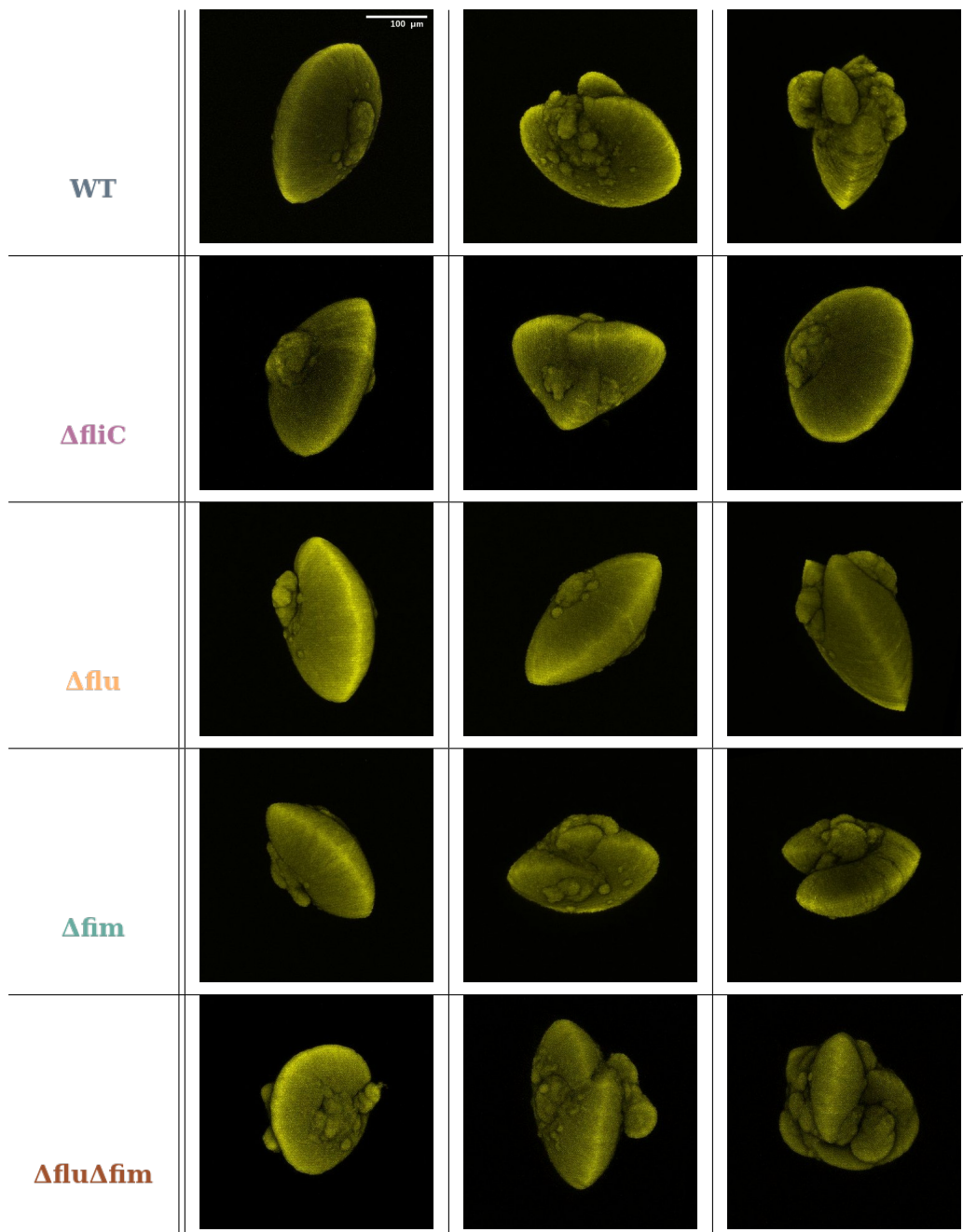
Table 8: Colonies at 0.6% Agar concentration. The table shows maximum intensity Z-projections of colonies imaged after 15 h of incubation time. There are three colonies per strain and the scale is the same for all images.

In this conditions, table 8 shows that it is difficult to find spherical colonies, most of them look elongated. On the other hand, the colonies present an almost uniform surface. If protuberances appear in the colonies the elongated shape is lost and the surface becomes more irregular, as seen in the third column of ΔfluΔfim. It seems that the stiffer the media the more elongated the colonies become. This result has been previously introduced in section 5.3.1, where other studies found lenticular colony shapes at high agar concentrations. In this project the elongated shapes are mostly seen at 0.6% (w/v) but they also appeared in some 0.5% (w/v) plates meaning that between these two concentrations should be a critical value where colonies change its behaviour.

In this case it is also difficult to tell apart colonies from different strains so they are also quantified. Even though the number of samples is small a T-test between parameters are perform under a significance of $\alpha = 5\%$.

In this case the biggest values of **Energy** corresponds to the double mutant, ΔfluΔfim and the smallest mean is found in the WT strain. The box plot for the energy can be found in figure 18. The **Entropy** box plot can be seen in figure 21, the biggest mean value corresponding to WT and the smallest to the double mutant ΔfluΔfim. In the last textural parameter, figure 24, the maximum **Homogeneity** mean corresponds to ΔfluΔfim and the smallest to WT. Table 13 contains the results of the T-test for the textural parameters. From this it is clear that the strain ΔfluΔfim is significantly different from the rest. Moreover, the strains WT and Δfim can be considered different.

When looking at the **Aspect ratio** box plot in figure 27 we can see how all the means are further from one than in the other agar concentrations. The most elongated colonies are Δflu and the least the ΔfliC. In the **Fractal dimension** box plot, figure 30 we can actually observe some differences between strains, with the most uniform strain being Δflu and the least ΔfliC. The results of the T-test for the volumetric parameters can be seen in table 14, from the aspect ratio values we see how none of the strains are statistically different. When comparing the fractal dimension Δfim and ΔfluΔfim can be considered different as well as ΔfliC and Δflu.
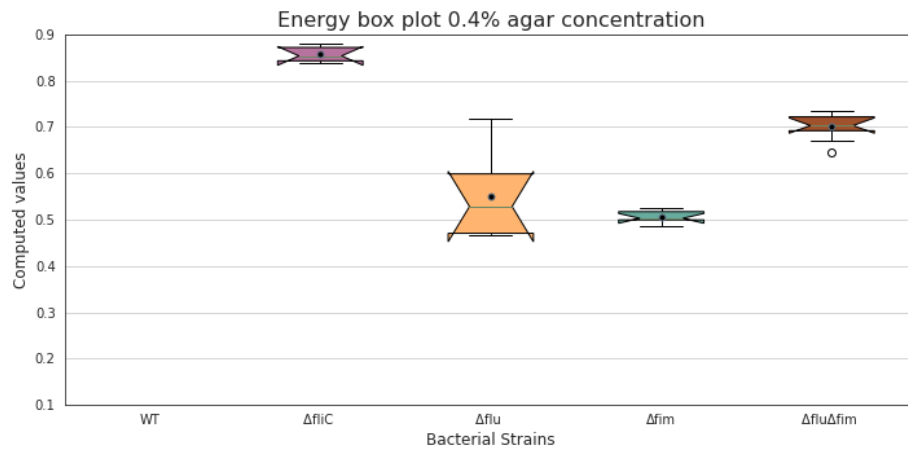
Figure 16: Energy box plot for the five strains at 0.4% agar concentration. Values computed for colonies growing for 15 h in M63 minimal media. The wild type strain values are not included since they did not form colonies at this concentration, the WT bacteria was found spread in the media.
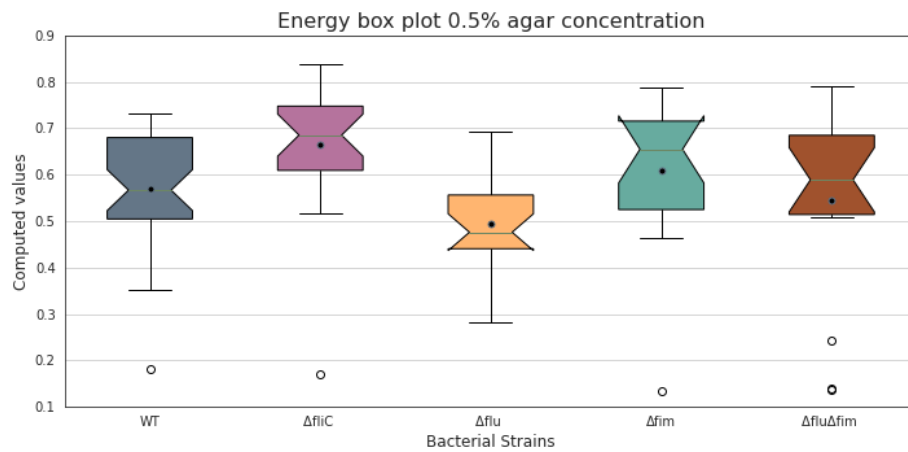
Figure 17: Energy box plot for the five strains at 0.5% agar concentration. Values computed for colonies growing for 15 h in M63 minimal media.
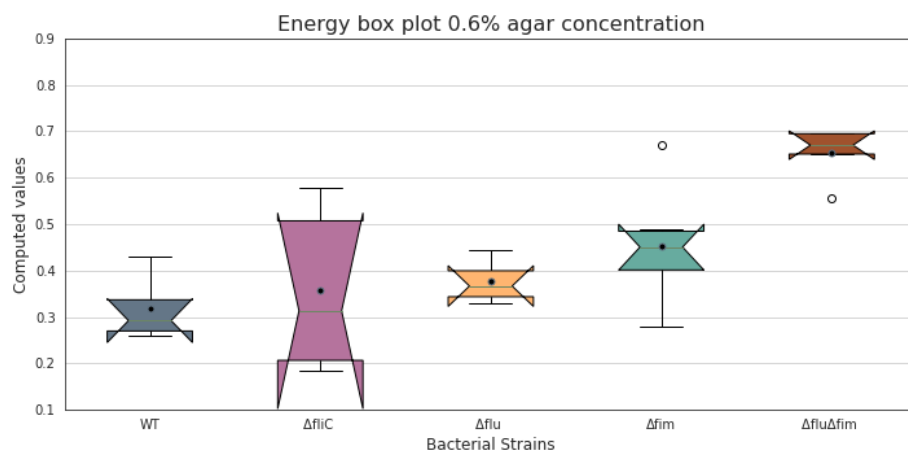
Figure 18: Energy box plot for the five strains at 0.6% agar concentration. Values computed for colonies growing for 15 h in M63 minimal media.
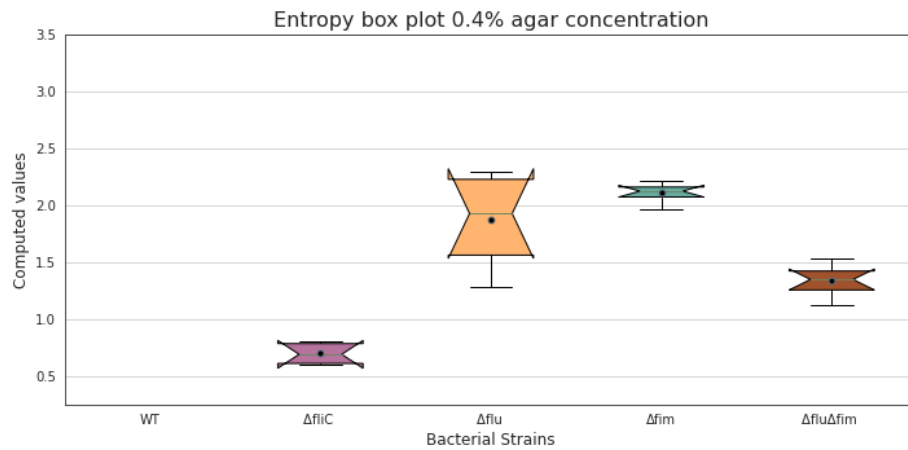
Figure 19: Entropy box plot for the five strains at 0.4% agar concentration. Values computed for colonies growing for 15 h in M63 minimal media. The wild type strain values are not included since they did not form colonies at this concentration, the WT bacteria was found spread in the media.
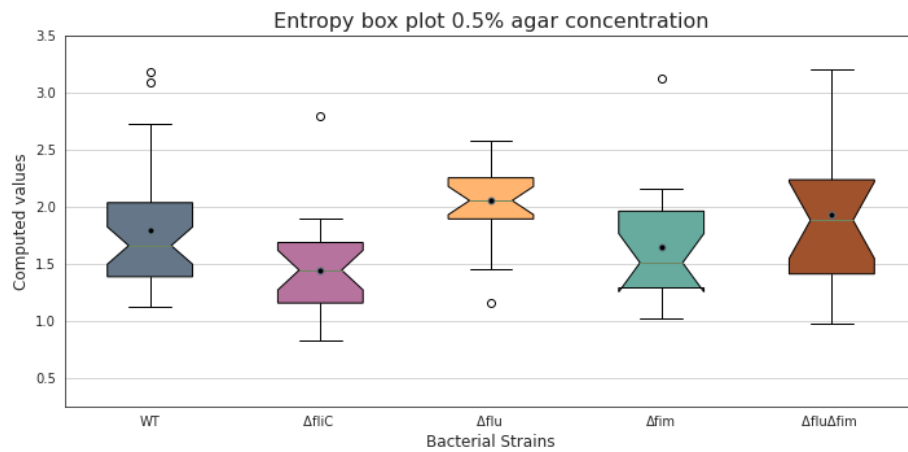
Figure 20: Entropy box plot for the five strains at 0.5% agar concentration. Values computed for colonies growing for 15 h in M63 minimal media.
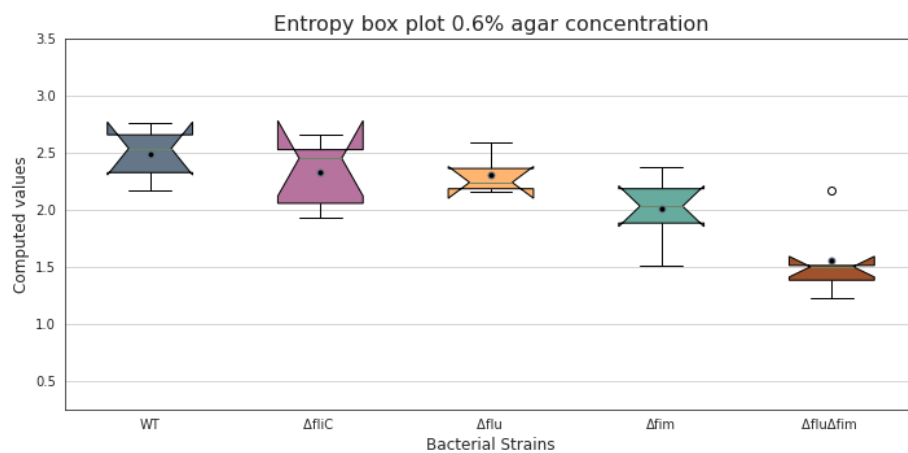
Figure 21: Entropy box plot for the five strains at 0.6% agar concentration. Values computed for colonies growing for 15 h in M63 minimal media.
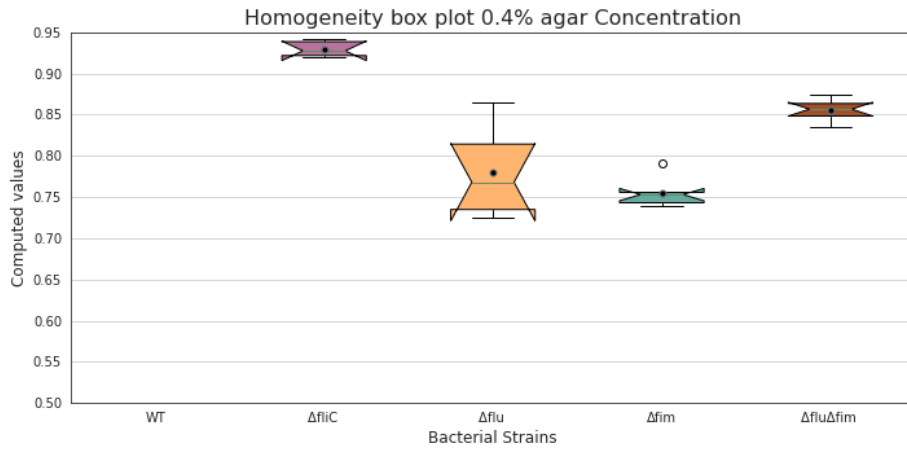
Figure 22: Homogeneity box plot for the five strains at 0.4% agar concentration. Values computed for colonies growing for 15 h in M63 minimal media. The wild type strain values are not included since they did not form colonies at this concentration, the WT bacteria was found spread in the media.
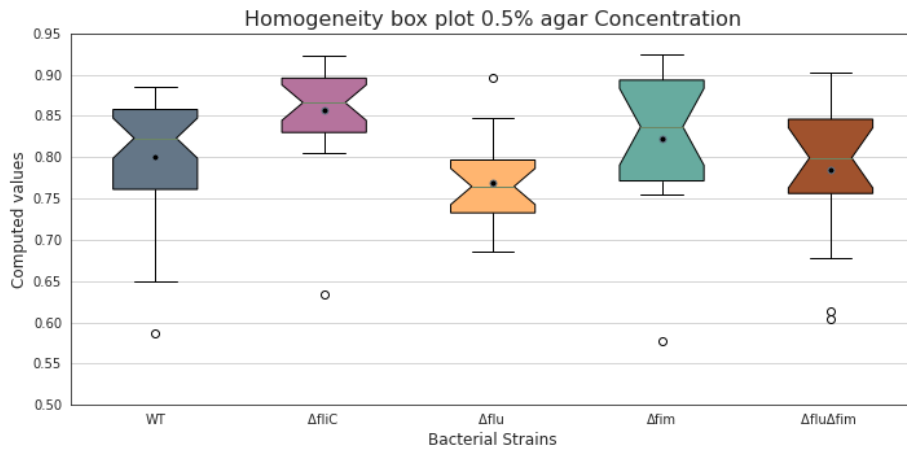
Figure 23: Homogeneity box plot for the five strains at 0.5% agar concentration. Values computed for colonies growing for 15 h in M63 minimal media.
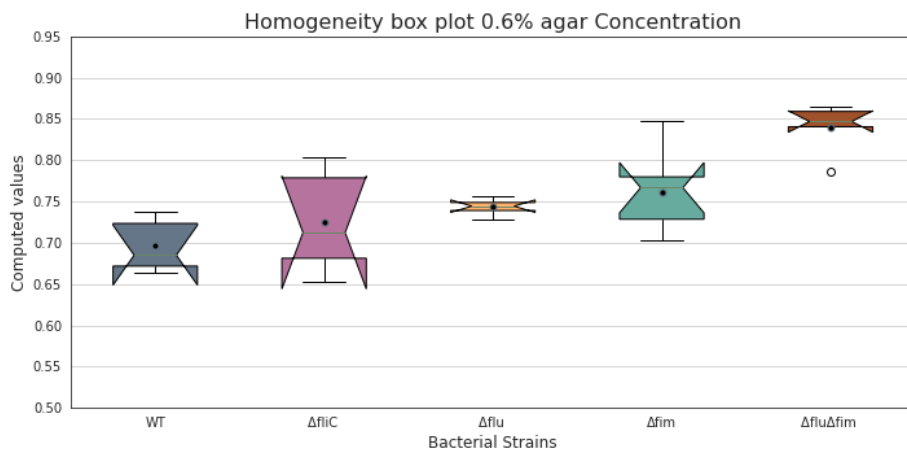
Figure 24: Homogeneity box plot for the five strains at 0.6% agar concentration. Values computed for colonies growing for 15 h in M63 minimal media.
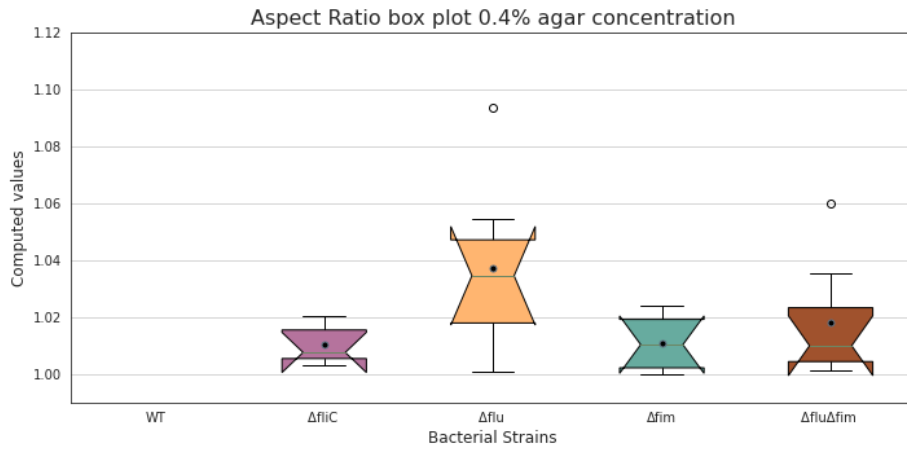
Figure 25: Aspect ratio box plot for the five strains at 0.4% agar concentration. Values computed for colonies growing for 15 h in M63 minimal media. The wild type strain values are not included since they did not form colonies at this concentration, the WT bacteria was found spread in the media.
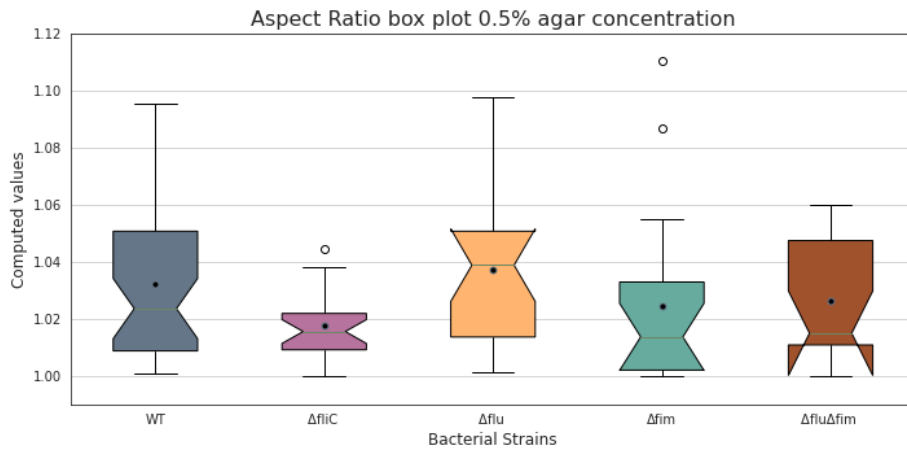
Figure 26: Aspect ratio box plot for the five strains at 0.5% agar concentration. Values computed for colonies growing for 15 h in M63 minimal media.
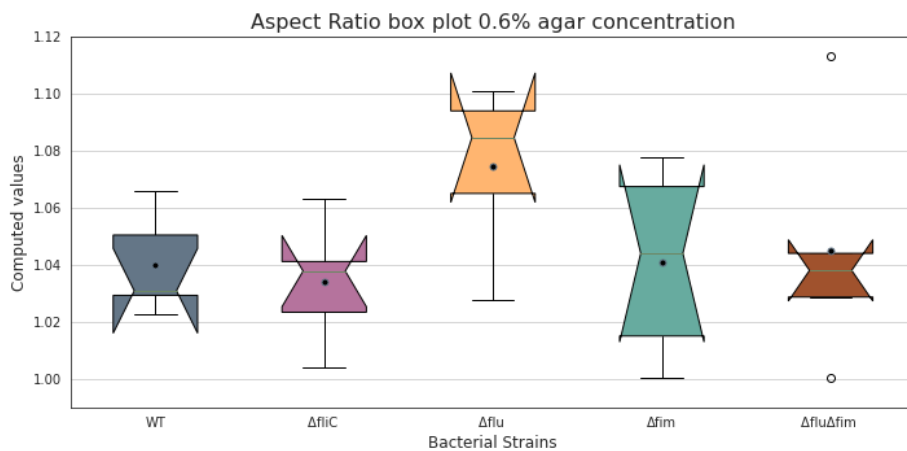
Figure 27: Aspect ratio box plot for the five strains at 0.6% agar concentration. Values computed for colonies growing for 15 h in M63 minimal media.
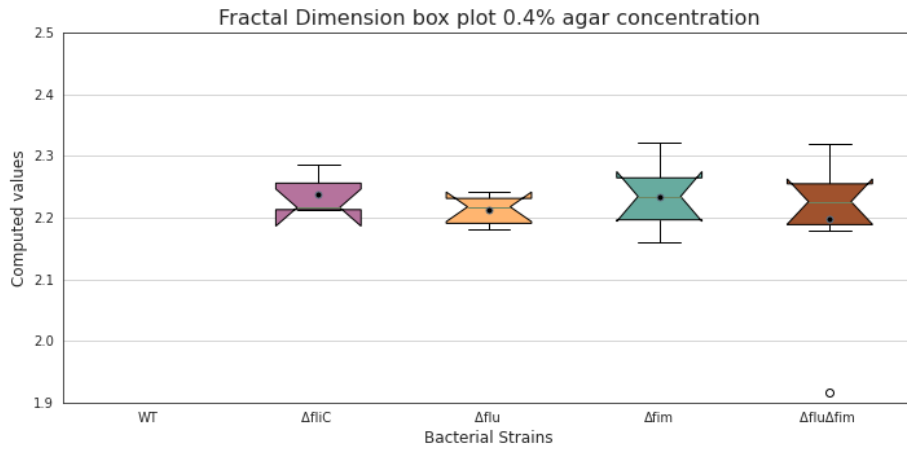
Figure 28: Fractal dimension box plot for the five strains at 0.4% agar concentration. Values computed for colonies growing for 15 h in M63 minimal media. The wild type strain values are not included since they did not form colonies at this concentration, the WT bacteria was found spread in the media.
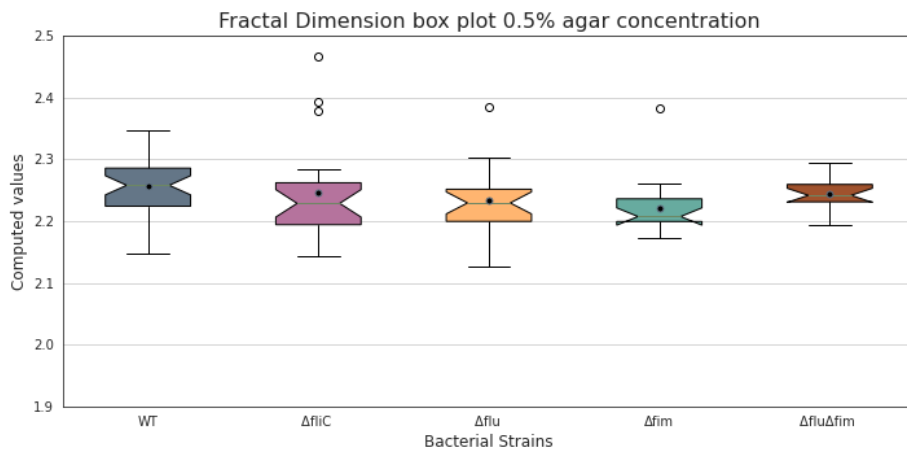
Figure 29: Fractal dimension box plot for the five strains at 0.5% agar concentration. Values computed for colonies growing for 15 h in M63 minimal media.
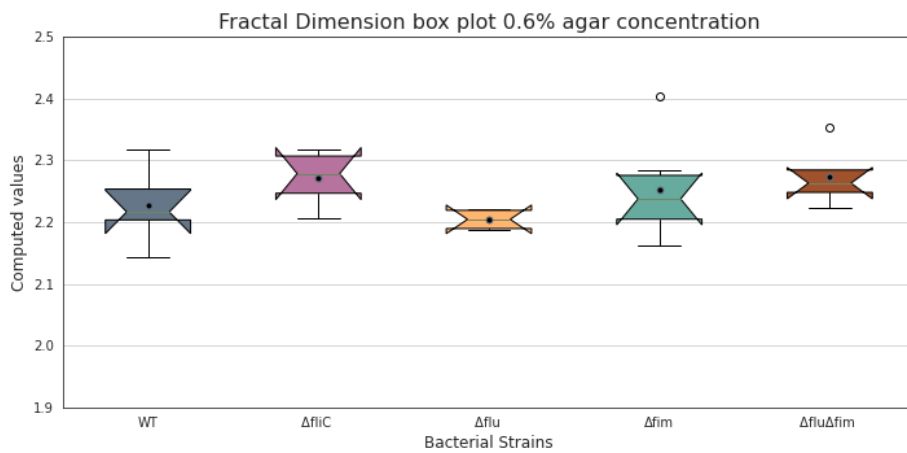
Figure 30: Fractal dimension box plot for the five strains at 0.6% agar concentration. Values computed for colonies growing for 15 h in M63 minimal media.

6.5   DISCUSSION

From this experiments two really interesting phenomena have been observed: the emergence of satellites in the wild type strain colonies growing at 0.5% agar concentration and a general elongation of the colony shape as the agar concentration increases. Even though the mechanisms behind them are not fully understood what is evident is that in a really narrow range of agar concentrations the bacteria, specially the WT strain, undergo a lot of processes that change the overall morphology of the three-dimensional colonies. So, for example the more elongated colonies observed at 0.5%(w/v) agar can have an origin in fluctuations that increased the agar concentration. Contrarily, we can think that the satellites emerge when this fluctuations reduce the local agar concentration and some of the cells are allowed to move.

A simple way to look for fluctuations can be to compare the aspect ratio of colonies growing on different days at 0.5% agar concentration as it is the parameter that gives a faster visual identification of elongated shapes. In this case fluctuations between colonies can appear from random errors during the experimental process such as the preparation of the media mixture. In figure 31(a) the aspect ratio values computed for wild type colonies growing on different days is shown. Values greater than 1.06 are not commonly found, but when they happen colonies with values really close to one are also observed in the same day, meaning that the fluctuations are as likely to happen between different days as between different Petri dishes prepared with the same media mixture. Figure 31(b) shows the aspect ratio computed for wild type colonies growing in the same plate. In this case, the three plates were produced with the same bottle of media and differences between aspect ratios are seen not only in colonies from different plates but in colonies from the same plate. If the aspect ratio value is considered to be directly correlated to the media stiffness, it is clear that fluctuations of the last appear locally in the Petri dishes. Therefore the final stiffness of the Petri dishes is a parameter difficult to control in the current experimental setup.

(a) Aspect ratio WT different days

(b) Aspect ratio WT different plates
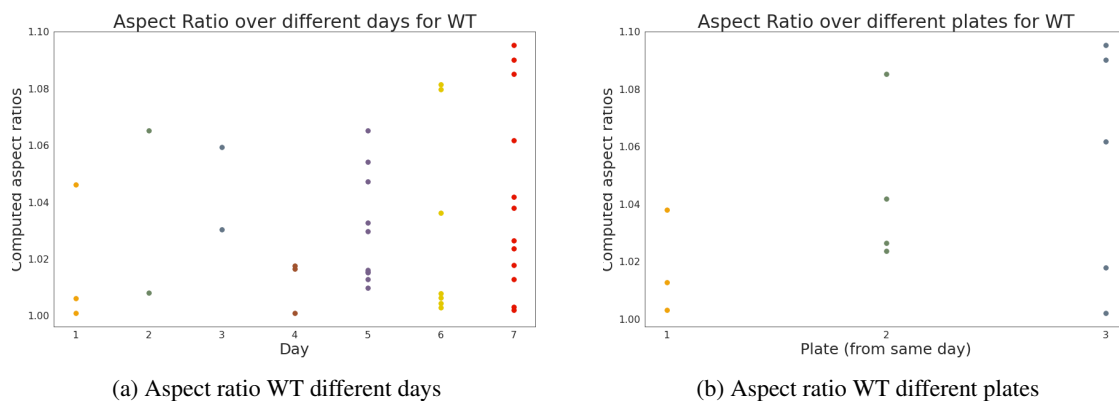
Figure 31: Values of the aspect ratio computed for WT colonies growing in M63 minimal media and 0.5% agar concentration for 15 h. (a) Each vertical line of dots shows the values obtained from colonies that come from the same experiment day. (b) Each vertical line of dots shows the values obtained from colonies that come from the same plate. The three plates compared are from the same experiment day.

Since the agar concentration has a important effect in the shape of the colonies, it is worth to perform an statistical test to see if the populations of the same strain growing under different conditions can be distinguished from each other. All the results of the T-test can be seen in appendix H in tables 15

and 16. The number of imaged colonies growing at 0.4% and 0.6% is always smaller than ten for all the strains. The results of the statistical test should be read really carefully as the data sets are small. From the numerical values what we can interpret is that mainly the textural parameters tell that a same strain is statistically different from itself when growing under different conditions. The volumetric parameters do not show this difference as often.

A result that repeats itself over all the agar concentrations is that the colonies of the mutant that presents a deletion in the gene encoding antigen 43, Δflu, are the ones with biggest aspect ratio. An hypothesis of why this happens can be proposed. This mutant does not express a handshake protein really important to cell-cell aggregation, therefore the bacteria in this colonies would be allowed to grow more freely giving place to structures that differ from the spherical shape with greater frequency.

In general the parameters seem to work well to distinguish the colonies from different strains at 0.5%(w/v) agar where there is the largest available data set. However, the doubt whether the fractal dimension is being appropriately determined could be easily solved by imaging the colonies with another objective, at the moment we work with an *NplanL20x0.40NA* objective because the fluorescence emitted by the cells is not great enough to use objectives with greater magnification. The maximum lateral resolution achievable can be computed with equation 2:

$$d = \frac{1.22\lambda}{2NA} = \frac{1.22 \cdot 514 \; nm}{2 \cdot 0.4} = 783.85 \; nm \tag{16}$$

If a *40x0.55na* objective could be used the lateral resolution would change to:

$$d = \frac{1.22\lambda}{2NA} = \frac{1.22 \cdot 514 \; nm}{2 \cdot 0.55} = 570.07 \; nm \tag{17}$$

The change between lateral resolutions is significant, so if after imaging the same colony with two different objectives the computed fractal dimension changes between images we could conclude that in this project there has been a limitation when estimating this parameter. Martin Møller Larsen [53], who worked in a similar project, imaged colonies of a certain bacterial strain with different objectives and found differences between the mean values of the computed fractal dimensions. Despite that, the same colony was not imaged with different objectives so it cannot be assumed that the limitation really exists.

7

LATTICE MODELS

A lattice model is a physical model defined on a lattice as opposed in the continuum of space. Lattice models are quite popular to perform computational simulations. In this project a lattice model, whose starting point is the Eden growth model, is proposed to understand how the morphology of the colonies behaves.

7.1 EDEN GROWTH MODEL

The Eden growth model is a lattice model that describes the growth of specific types of clusters such as bacterial colonies. The model, named after Murray Eden was first described in 1961 [54] and in three dimensions forms radial clusters with irregular fractal borders. It is a benchmark of stochastic processes, in the important class of growth models on expanding substrates. In this model, new cells are irreversibly added at random positions of the neighborhood of previously existent cells placed on a stationary square lattice, a diagram showing this process can be seen in figure 32.

7.1.1 *Implementation*

The algorithm followed to implement the Eden Growth Model in three dimensions is described in algorithm 1.
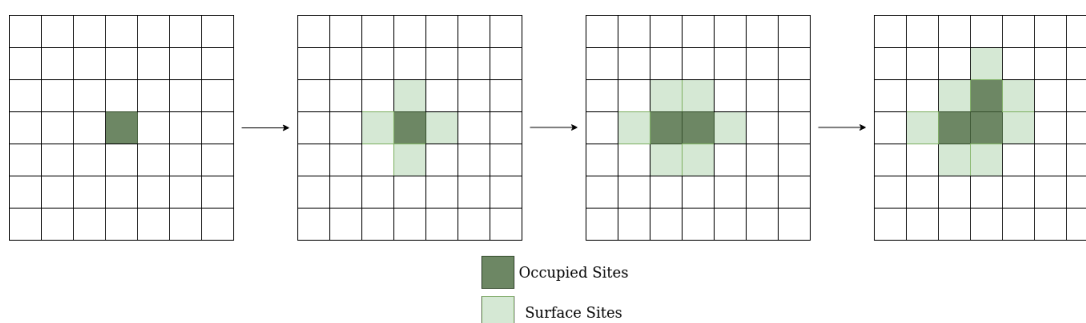
Figure 32: Diagram showing how the Eden Growth Model is implemented in a two-dimensional square lattice. The dark green squares represent occupied sites and the light green squares the available growth positions. The black arrows show the evolution over time. At first one occupied site is in the center of the lattice, in the second figure its available growth sites are found and one of those is chosen randomly. In the following time step, the lattice presents two occupied sites, again its available neighbours are found and one of them is chosen randomly as a growth position. The process can continue as many times as wanted.

Algorithm 1: 3D Eden Growth Model

Input: Lattice size L, Average division time τ and the total number of events P

Result: Aggregate of P cells in a 3D lattice

1 Generate a 3D lattice of dimension L. With empty sites $Lat(i, j, k) = 0$, and occupied sites $Lat(i, j, k) = 1$;

2 Place a single cell in the center of the lattice;

3
$$Lat\left(L/2, L/2, L/2\right) = 1$$

for $p \leftarrow 0$ **to** P **do**

4   Define an empty colony surface S;

5   **foreach** *occupied site* $Lat(i, j, k) = 1$ **do**

6   Find the number of empty near neighbours, $Lat(i \pm 1, j, k) = 0$, $Lat(i, j \pm 1, k) = 0$ and $Lat(i, j, k \pm 1) = 0$;

7   And add their lattice position to the surface of the colony S;

8   **end**

9   Chose a random surface site $S(m, n, l)$ and update the colony by setting a cell in that position $Lat(m, n, l) = 1$.;

10   Find the average time of the interval;

11
$$\Delta t = \frac{\tau}{\sum_{ijk}(Lat(i, j, k) = 1)}$$

12 **end**

7.1.2 *Modifications to the Eden Growth Model*

Even though the Eden growth model presents a lot of applications in many systems there is no full theoretical understanding of it. The model can be modified in order to describe certain scenarios better, this can be done introducing new parameters such as:

- A probability that is assigned to the available growth sites. So in one event each available site has a probability p of being linked to the aggregate. This modification produces an effect similar to a multiple selection process.

- A sticking probability, at each event a single surface site is selected with probability s to join the aggregate. This parameter does not affect the overall morphology of the aggregate but can vary the timescale of the process.

- A noise reduction parameter, where a certain surface site needs to be chosen m times before joining an aggregate.

However, the Eden cluster obtained in all cases will be anisotropic due to the underlying lattice, its shape tends to lengthen along the directions of the lattice axes. Eden simulations on a square lattice have revealed a distortion away from a circular shape towards a diamond shape with increasing N

[55]. This effect is specially remarkable when working with a noise reduction parameter. To solve this some off-lattice models have been proposed where the cluster is composed of touching circles instead of squares [56]. In this project we are far from observing this anisotropies, so it is considered that working with an on lattice model is pertinent for the study.

7.2 MODEL WITH SWIMMERS

From the experimental results in chapter 6 a wide range of colony morphologies are observed under different conditions and two peculiar phenomena are reported. A transition between almost spherical colonies and more elongated ones, seen as the agar concentration of the media increases, and the emergence of satellites in colonies of the wild type strain growing in 0.5% (w/v) agar. In this section a new modification of the Eden growth model is proposed to describe how the satellites can appear in the experimental colonies. It is a really naive approximation that does not include many parameters but can provide a first description to more complex studies.

The purpose of the model is to exclusively describe how the satellites can appear. Despite the mechanisms behind this phenomena being not clear at the moment, it is assumed as a direct consequence of bacterial motility, swimming in particular. It is proposed that some cells are able to swim far away from its generation position in the lattice. Meaning that, bacteria in the colony can divide and increase the size of the aggregate or can detach from it and stick to a new position where they can grow and divide, forming another aggregate.

To simulate this behaviour in a three dimensional squared lattice the number of empty neighbours, is to say the available growth sites, of each bacteria is the parameter chosen to determine whether a cell can swim or not. As in the Eden growth model, bacteria with no available neighbouring sites can not grow and in this model neither swim. There are two types of bacteria in the system:

- Type 1: cells with one, two or three available neighbouring sites (N_1), they are only allowed to grow at a certain rate, k.

- Type 2: cells with more than three available neighbouring sites (N_2), can growth at rate k or swim at rate k_s.

When a type 2 cell is chosen to swim three random numbers that follow a Gaussian distribution are thrown. These determine the new position of the cell respect its original site. The Gaussian distribution followed is the same for all three directions of growth (x, y and z):

$$P(x) = \frac{1}{\sqrt{2\pi\sigma_x^2}}e^{(-x^2/2\sigma_x^2)}; \quad P(y) = \frac{1}{\sqrt{2\pi\sigma_y^2}}e^{(-y^2/2\sigma_y^2)}; \quad P(z) = \frac{1}{\sqrt{2\pi\sigma_z^2}}e^{(-z^2/2\sigma_z^2)}; \quad (18)$$

Where $\sigma_x = \sigma_y = \sigma_z = \sigma$. This three distributions can be expressed as a radial distribution that gives the total distance the bacteria moves from its position in the main aggregate:

$$P(r) = \frac{4\pi r^2}{\left(\sqrt{2\pi\sigma_3^2}\right)^3}exp\left(\frac{-r^2}{2\sigma_3^2}\right) \quad (19)$$

With $\sigma_3 = \sigma$. This radial distribution is slightly different than a Gaussian distribution as can be seen in figure 33.
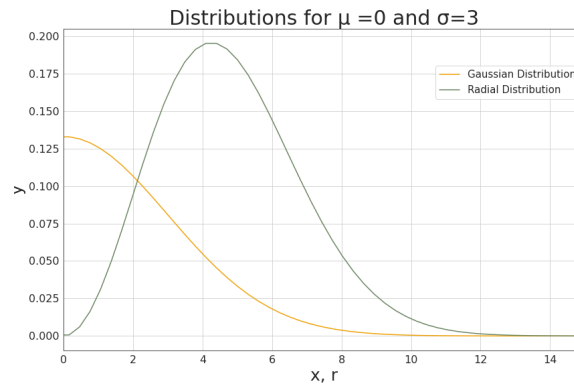
Figure 33: Plot with the Gaussian distribution that the random numbers thrown to decide the distance jump in each direction follow and the radial distribution that describes the final distance a cell swims. Both are plotted for the same mean and standard deviation.

In many studies swimming is described as a run and tumble process [57] where bacteria follow a random walk trajectory. In this model the swimming process is coded like a jump. That is because the exact time-scale of each process for bacteria growing in semi-solid media are not known, but the movement is assumed to happen faster than the growing. Therefore, having a final random position after one event is equivalent to having the final position after many steps of a random walk that would occur in a shorter time-scale.

At the end this modified model introduces two parameters that can deviate the cluster behaviour from the typical Eden cluster: the swimming rate, k_s, and the standard deviation of the Gaussian distribution, std.

7.2.1 *Implementation*
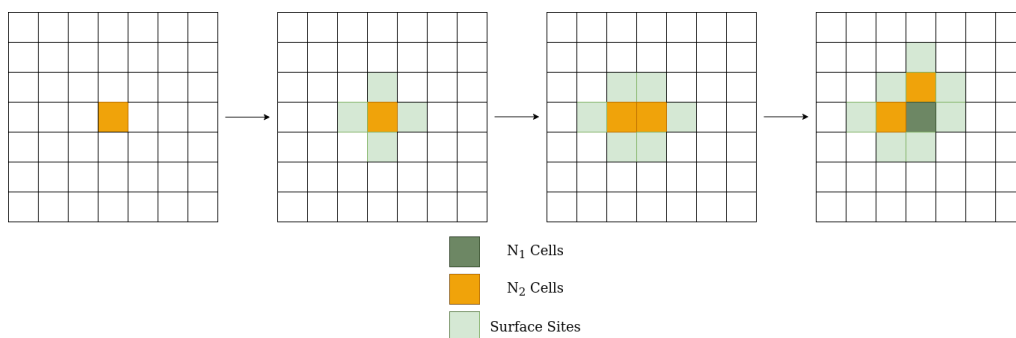
Figure 34: Two-dimensional representation of the Eden growth model with swimmers. In this case the cells allowed to swim have to present more than two available neighbouring growing sites. The cells that can swim or grow are represented in orange, while the ones that just can grow in dark green. The available growth sites appear as light green squares and the black arrows show the evolution over time. In this example none of the cells are chosen to swim since the event presents a really low probability of happening.

A diagram of the model can be seen in figure 34 and its implementation appears in algorithm 2. An event driven approach is followed where the time of each event is estimated from the event rate. For simplicity the growth rate is defined as $k = 1$, so it is easier to find how changes in the swimming rate k_s affect the final aggregate morphology.

Algorithm 2: 3D Eden Growth Model with swimmers

Input: Lattice size L, growth rate k, swimming rate k_s, standard deviation std and an average $\mu{=}0$ of a Gaussian distribution and the total number of events P

Result: Aggregate of cells in a 3D lattice

1 Generate a 3D lattice of dimension L with empty sites $Lat(i, j, k) = 0$ and occupied sites $Lat(i, j, k) = 1$;

2 Place a single cell in the center of the lattice

$$Lat\left(L/2, L/2, L/2\right) = 1$$

for $p \leftarrow 0$ **to** P **do**

3   Define an empty colony surface, S;

4   Define an empty swimmers array, $swim$;

5   Set the number of each cell types, $N1$, $N2$ to zero;

6   **foreach** *occupied site* $Lat(i, j, k) = 1$ **do**

7   Find and count the number of empty near neighbours β

$$Lat(i \pm 1, j, k) = 0 \quad Lat(i, j \pm 1, k) = 0 \quad Lat(i, j, k \pm 1) = 0$$

     Add the available sites position to the surface of the colony S.

8   **if** $\beta > 3$ **then**

9   Add an element to $N2$;

10   Save the cell position in $swim$;

11   **else if** $0 < \beta \leq 3$ **then**

12   Add an element to $N1$;

13   **end**

14   Find the total event rate $T = N1 \cdot k + N2 \cdot (k + k_s)$;

15   Determine which event happens at time $t = -ln(r)/T$, with $r = U \subseteq (0, 1)$, by trowing a random number from an uniform distribution $a = U \subseteq (0, 1)$;

16   **if** $(N1 + N2) \cdot k/T < a$ **then**

17   Chose a random surface site $S(m, n, l)$ and update the colony by setting a cell in that position $Lat(m, n, l) = 1$;

18   **else**

19   Throw three Gaussian numbers to determine the final position of the cell:
$x_g = P(x) \quad y_g = P(y) \quad z_g = P(z)$;

20   Select an element of the swimmers array $Lat(m', n', l')$;

21   **if** $Lat(m' + x_g, n' + y_g, l' + z_g) = 0$ **then**

22        $Lat(m', n', l') = 0$;

23        $Lat(m' + x_g, n' + y_g, l' + z_g) = 1$;

24   **else**

25   Go to 19;

26   **end**

27   **end**

28 **end**

<div style="text-align: right; font-size: 3em;">8</div>

SIMULATION RESULTS

In this chapter the results obtained with the Eden growth model that includes swimmers are shown.

8.1 EDEN GROWTH MODEL WITH SWIMMERS

As previously stated in section 7.2, we end up with a model that has two free parameters k_s and std. The probability of swimming, k_s, defines the rate at which the cells allowed to move will do it compared to its growth rate. The standard deviation of the Gaussian distribution, std, establishes the variance of the distribution the bacteria follow when they are chosen to move, therefore it determines the final position of the swimmer cells after one swimming event.

In agreement with the experimental results, where swimming is a rare event, k_s is given small values for all the simulations. It is also known that the satellites do not move really far away from the main colony, at least the ones that can be imaged, so std should be given small values accordingly.

With an 20x objective the size of the experimental images were 512x512 pixels in the x, y directions. In order to reproduce the observed colonies the lattice size in the simulation is set to 500x500 sites. Aiming to conserve the symmetry of the final colony the z direction also has 500 sites, even though in the experimental files it corresponded to the number of stacks, which is much smaller.

The final step before launching the simulations is to decide after how many iterations we want to look at the shape of the colony. Since we do not know the exact doubling time of the cells when growing embedded in a semi-solid media we can roughly estimate the number of cells in a colony by looking at the size of the experimental ones. The colonies observed usually presented a ratio in the scale of 100 μm, so assuming a spherical shape the volume of the colonies is in the order of 10^6 μm^3 and the volume of an *E.coli* cell can be approximated to ≈ 1 μm^3 [58], therefore each colony contains around a million cells. Since the bacteria in the model can grow or swim there are two possible events per iteration. Regardless the small swimming probability the colony morphology is checked after 1.5 million of events, to ensure that in silico colonies reach a million of cells for all the different combinations of parameters.

First the code is run for five different swimming rates, $k_s = 0.01, 0.02, 0.1, 0.15$ and 0.2, and five different standard deviations, $sdt = 2, 3, 5, 7$ and 10 to have an overview of how the colony morphology changes.

	ks = 0.01	ks = 0.05	ks = 0.1	ks = 0.15	ks = 0.2
std = 2					
std = 3					
std = 5					
std = 7					
std = 10					
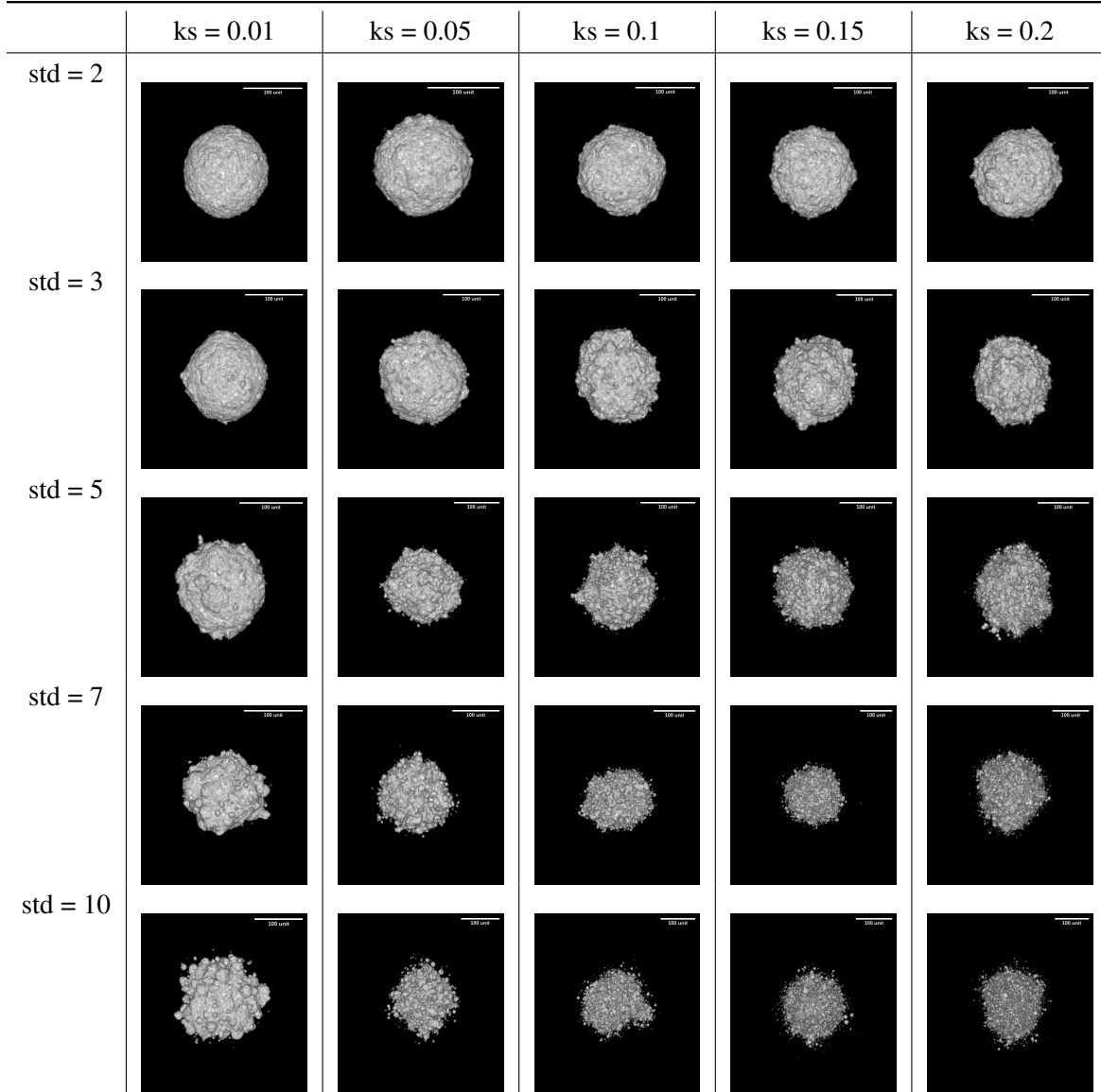
Table 9: In silico results showing 25 colonies obtained from running the code with different standard deviations and swimming rates. Since the three-dimensional reconstruction is done with a plugin [47] included in FIJI that sets the best dimension to show the colony a scale bar of 100 units, is to say, lattice sites is included at each image. At small swimming rates and standard deviations the colonies look almost spherical and compact. When these parameters increase the symmetry starts breaking and satellites emerge. These changes are seen faster when increasing the standard deviation rather than when the swimming rate increases.

In table 9 a three dimensional reconstruction of the colonies obtained with the model can be seen. Basically, two types of aggregates are formed. The first ones appear at low swimming probabilities and short jump distances. These colonies are single aggregates without satellites, as can be seen for the parameters $k_s = 0.01 - std = 2$ or $k_s = 0.01 - std = 3$. The second type of clusters are colonies that present satellites, as can be seen in $k_s = 0.01 - std = 10$. The bigger the parameters become the more satellites are formed, until the aggregates obtained do not look as a single colony anymore, as happens in $k_s = 0.2 - std = 10$. Since the model is stochastic some parameters can lead to both colony types, this happens for example at $k_s = 0.01 - std = 5$.

(a) Slice after 10^4 events   (b) Slice after 10^5 events   (c) Slice after 10^6 events   (d) Slice after $1.5 \cdot 10^6$ events
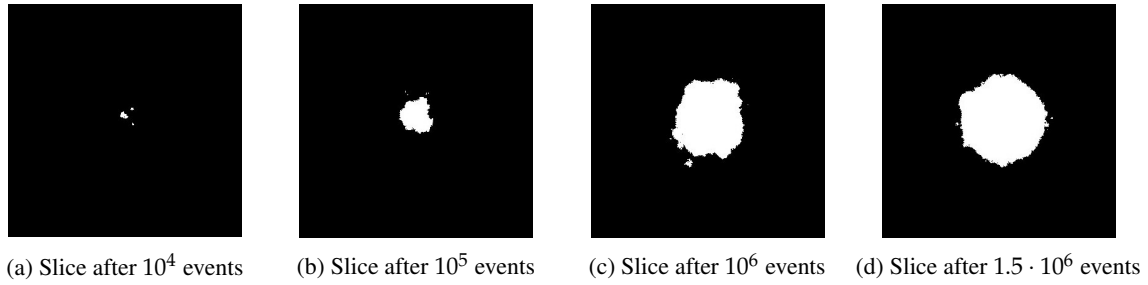
Figure 35: Time evolution of the same cross-section from an in silico colony after a certain number of events when the parameters are set at $k_s = 0.01$ and $std = 7$. Looking at the results of table 9 is expected that the colony presents satellites at the end of the simulation.

In figure 35 four snapshots of the same cross-section of a colony growing at $k_s = 0.01$ and $std = 7$ are presented. Depending on the number of events it presents satellites or not. In the first image, 35(a) there is a colony with two satellites of a considerable size. After some time, figure 35(b), these satellites are merged with the main aggregate. In the third snapshot, 35(c), a satellite can be seen but this is again incorporated to the colony in the last figure 35(d). This result shows the importance of comparing the colonies after the same number of events, because different parameters can lead to the same results if the simulations run for different number of iterations. To observe satellites the typical swimming distance should be bigger than the aggregate size, otherwise the cells that escape the surface will be quickly incorporated to the main colony, as can be seen for all the colonies obtained when setting the standard deviation to 2 that do not present any satellites.

Having two different processes it is interesting to look at how the number of cells evolves in systems with different parameters. The effect of changing the swimming rate when the standard deviation is fixed and vice-versa is studied.

(a) Linear scale evolution   (b) Semi-logarithmic scale evolution
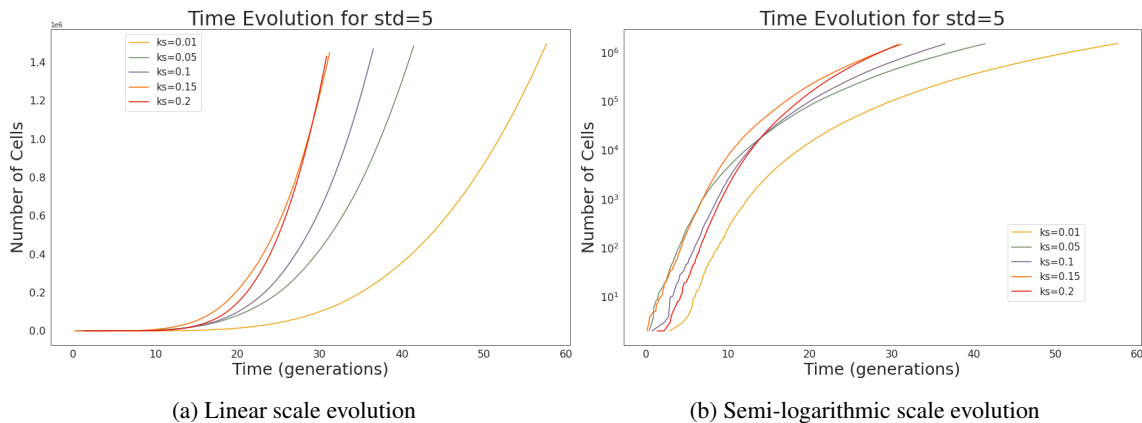
Figure 36: Figure showing the evolution of the number of cells over time in systems with different swimming rates, the higher the k_s the more exponential is the growth. (a) Shows evolution in linear scale. (b) Shows evolution in semi-logarithmic scale.

(a) Linear scale evolution   (b) Semi-logarithmic scale evolution
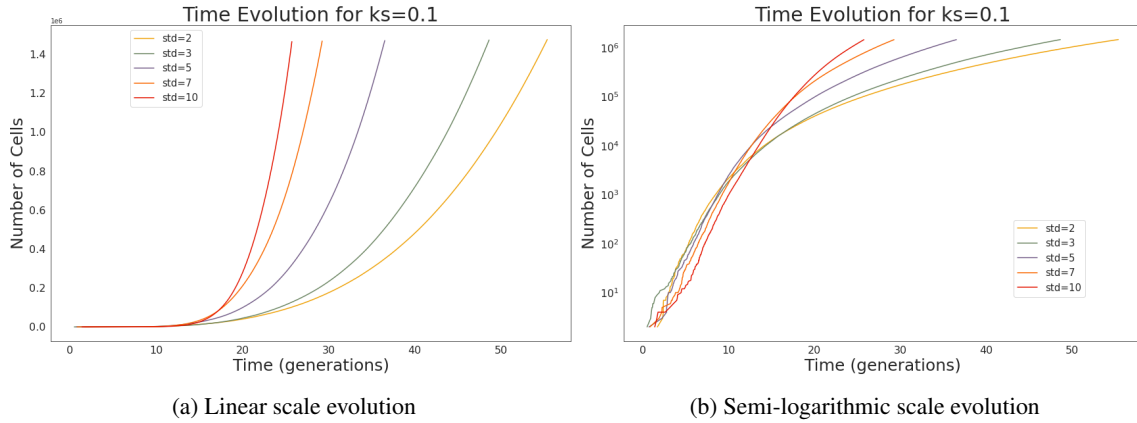
Figure 37: Figure showing the evolution of the number of cells over time in systems with different standard deviations, the bigger the std value the more exponential is the growth.(a) Shows evolution in linear scale. (b) Shows evolution in semi-logarithmic scale.

In figure 36 the number of cells over time is plotted for systems that present the same standard deviation, $std = 5$ but different swimming rates. There is a clear tendency where the higher the rate the more exponential is the growth of the system. In figure 37 the number of cells over time is plotted for systems that present the same swimming rate, $ks = 0.1$ but different standard deviations. The higher the rate the more exponential is the growth of the system. Despite the figures showing a similar behaviour when looking at the semi-logarithmic plots in figures 36(b) and 37(b) it is evident how an increase in the standard deviation has a bigger effect that changes in the swimming rate.

The behaviour of the evolution can be easily explained by looking at the nature of the Eden growth model, it starts as an exponential growth, but over time this growth becomes linear since only the surface of the aggregate is able to grow. The introduction of swimmers modifies this behaviour by generating new occupied sites in the lattice without empty neighbours that can grow exponentially. So, an increase in the swimming rate will increase the number of aggregates that can grow quickly. By contrast, increasing the standard deviation makes the motile cells move further away from the surface of the main colony. Meaning that it takes more time for the different aggregates to merge, therefore, there are different surface clusters growing for longer time.

8.2   COLONY QUANTIFICATION

In section 8.1 some values of swimming rates and standard deviations lead to colonies that presented satellites after 1.5 million of events. Some of the parameters combinations always gave colonies with satellites, on the other hand other parameters generated colonies that never presented satellites. Lastly, there were parameters whose resultant colonies fluctuated between both states. In this section some colonies generated targeting each of the previous mentioned cases are quantified. Since the simulation returns a binary stack of images, only the volumetric parameters can be computed. The swimming rate is set at $k_s = 0.01$ and three standard deviations are compared, $sdt = 3$ that gives no satellites, $std = 7$ that always gives satellites and $sdt = 5$ that oscillates between states.

In figure 38 the box plot of the aspect ratio is showed. All the values are really close to one, meaning that the spherical shape of the colonies is not highly disrupted, but the bigger the std the

bigger the values of the aspect ratio become. A T-test between parameters can be performed with a significance of $\alpha = 5\%$, the results of which appear at table 10. All the simulations are statistically different from each other. This result changes when looking at the T-test between the fractal dimension values. In figure 39 the box plot for the fractal dimension is shown, the bigger the swimming distance the more irregular is the surface of the colony. This makes sense if the protuberances that appear are considered to be old satellites that are merged with the main colony as the number of events increases. The fractal dimension of $std = 3$ being equal to $std = 7$ could be explained by looking at the box plot of the first, whose distribution is not really normal compared to the others.
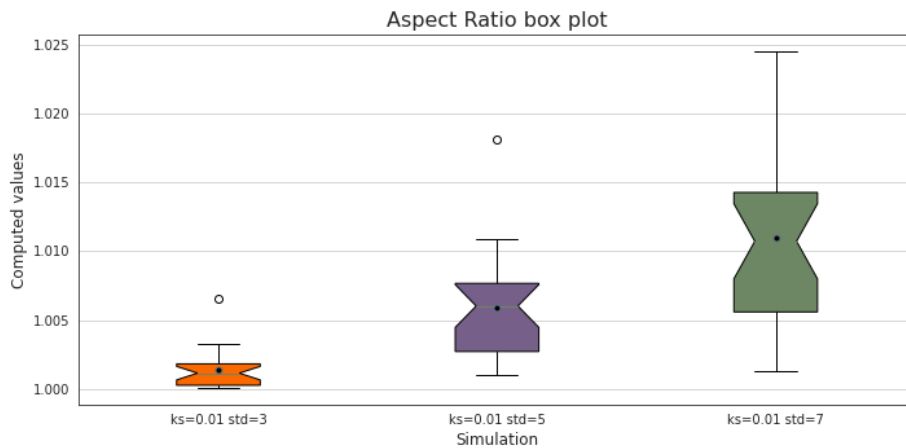
Figure 38: Figure showing the box plot of the aspect ratio computed for in silico colonies obtained with three different sets of parameters after 1.5 million of events. Each distribution is obtained with 30 in silico colonies.
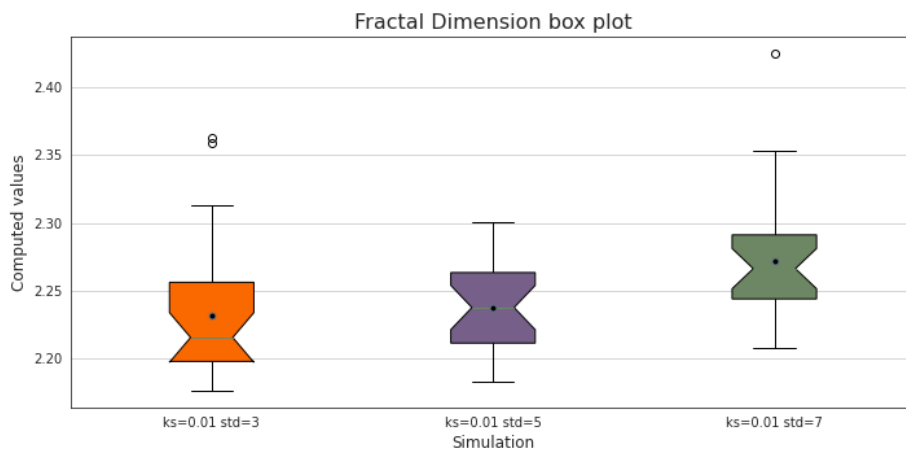
Figure 39: Figure showing the box plot of the fractal dimension computed for in silico colonies obtained with three different sets of parameters after 1.5 million of events. Each distribution is obtained with 30 in silico colonies.

$k_s = 0.01$	Aspect Ratio		Fractal dimension	
std / std	T_{val}	p_{val}	T_{val}	p_{val}
3 / 5	-3.34	0.0018	-3.069	0.0036
3 / 7	5.43	6.43e-06	0.444	0.658
5 / 7	7.13	1.31e-07	2.97	0.0046

Table 10: T-test of the volumetric parameters computed for in silico colonies.

8.3 DISCUSSION

In this naive model the emergence of satellites is observed. How these evolve over time begs the question if the deviations from the spherical shape observed in experimental colonies growing at 0.4%(w/v) and 0.5%(w/v) agar can be a consequence of motile bacteria that detached from the colony at earlier times. If the cells do not move really far from the colony surface these can be reabsorbed into the main colony as the aggregates grow.

The volumetrical quantification of the in silico colonies gives distribution of values compatibles for some of the experimental colonies after growing 15 in M63 minimal media in 0.4% and 0.5%, seen in figures 25, 26, 28 and 29. The general morphology of these colonies is also similar to the computational ones as can observed in figure 40 where a three-dimensional reconstruction of an experimental colony of the double mutant strain, after image processing, is next to a three-dimensional reconstruction of an in silico colony obtained with $k_s = 0.01$ and $std = 5$.

(a) Experimental ΔfluΔfim colony

(b) In silico $k_s = 0.01$ and $std = 5$ colony
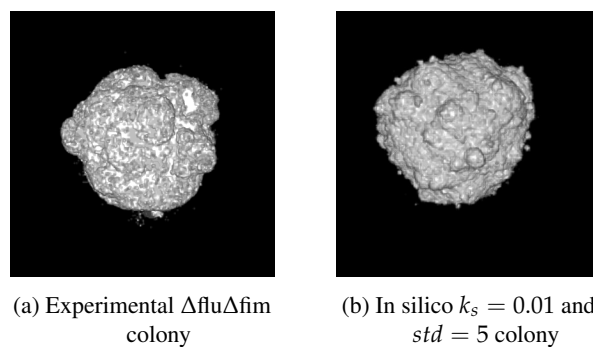
Figure 40: (a) Three-dimensional reconstruction of an experimental ΔfluΔfim strain colony after image processing. (b) Three-dimensional reconstruction of an In silico colony obtained with $k_s = 0.01$ and $std = 5$, half of the stacks were removed so the comparison with the experimental colony was more appropriate. Both colonies look as stochastic aggregates.

As the objective of this model was to reproduce one of the experimental phenomena observed there are many parameters that are not being included. One of the modifications the model, in order to obtain aggregates more similar to the experimental colonies, could be the introduction of a nutrient field that favours the motility of cells in a certain direction. Needless to say, the stiffness of the agar it is not considered in this system, so at any point the model was expected to reproduce the elongated colonies observed at 0.6% agar concentration. In general, it is a simple model that gives results easy to interpret and provides a starting point for more complex studies.

9

CONCLUSIONS

9.1 CONCLUSIONS

This thesis aimed to grow three-dimensional bacterial colonies and study its morphology. The experimental methods and the simulations lead us to some interesting conclusions.

Looking at the results of the different strains we can clearly separate the wild type behaviour from the mutants. The wild type strain is the only one that exhibits satellites in some of its colonies when growing at 0.5% agar concentration. How these satellites emerge remains unknown, but the results gathered in this study point to the phenomenon having an origin in bacterial motility. Apart from the wild type strain some of the mutants also express flagella which are thought to be the main responsible of bacterial motility. The mutant colonies not presenting satellites is compatible with the results of the motility assay at 0.5%(w/v) agar in M63 minimal media, displayed in section 6.1 where the wild type bacteria were the only cells able to move. To explain why there is such a difference between the motility of the strains two hypothesis can be proposed. In one of them the reduction of the motility of the mutants is seen as a consequence of an over-expression of some structures that block the normal production of flagella [50]. In the second it is said that other components, that could be deleted in the mutants, aside from flagella are important to achieve the most efficient motility mechanism.

At lower agar concentrations, 0.4% (w/v) agar, wild type bacteria did not grow as three dimensional colonies. However, the rest of strains formed aggregates of almost spherical shapes. The wild type strain becomes indistinguishable from the mutants when growing at 0.6% agar concentration. In this higher agar value all the strains give place to elongated colonies, which agrees with the lenticular colony shapes observed in other studies [43] and whose origin is not completely understood.

Therefore, we can say that the environment, the stiffness of the media in particular, seems to have a greater effect in the morphology of the colonies than the different properties between strains. This has been an interesting finding and the shapes variations have been observed in a really narrow range of agar concentrations. Which means that the changes in the shape between almost spherical and elongated colonies observed mostly in colonies growing at 0.5% agar concentration can have an origin in local fluctuations in the stiffness of the experimental plates .

The computational model proposed in this project seeks to reproduce the emergence of satellites observed in some of the experimental colonies growing at 0.5% agar concentration. In the model cells that can swim by performing a jump that follows a Gaussian distribution for each of the spatial directions are added to the Eden growth model. The introduction of swimmers is a really

naive approximation, nevertheless with it satellites form around the main cluster of cells. For the appropriate parameters these swimmers can also be seen as the origin of the protrusions that break the spherical shape in some of the colonies. If they remain close enough to the colony surface they are re-incorporated to the main aggregate causing a disruption in the almost uniform boundary of the colony.

Overall, the results obtained in this project provide a great starting point for new investigations focused in the different phenomena observed.

9.2 FUTURE WORK

This project leaves many unanswered questions that is worth to continue studying.

For future experiments it will be crucial to pay more attention to the properties of the semi-solid media to reduce the fluctuations in the agar concentration as well as the nutrient field. It will be also a good idea to test the stiffness of different nutritional media for a same agar concentration and see if there is any significant difference between them as some studies show [51].

To test if the fractal dimension of the colony was being correctly determined, an objective with bigger magnification is required. The strains of the project include a YFP plasmid whose intensity was not optimal, so if it is wanted to study the same strains it can be advantageous to transform the original ones to include a plasmid with better fluorescence.

Even though it has not been discussed that much, imaging the colonies with a confocal microscope just allows the visualization of half of the colony. This is an important limitation that should be overcomed to have a full understanding of the colony morphology.

To test if the satellites are a consequence of bacterial motility a time-lapse experiment could be performed. The results of this could also tell if the approach for the modelling with the introduction of swimmers in the Eden growth model is appropriate.

About the modelling, a lot of processes could be included into the simulation, such as a nutrient field that favours the swimming into a particular direction. A study concerning whether a lattice model is convenient to describe the colonies at higher agar concentrations where they present an elongated shape could also be done. It seems that the elongation has an origin in mechanical forces of the media acting against the colony, so other approaches where forces can be easily modeled should be also considered.

APPENDICES

<div style="text-align: right">

A

</div>

MEDIA PREPARATION

A.1 LYSOGENY BROTH: RICH MEDIA

Preparation of 100 ml of media.

1. Mix all the components:

   - 100 ml Milli-Q® Water

   - 1 g Bacto Tryptone

   - 0.5 g Yeast extract

   - 0.5 g NaCl

2. Measure the pH of the solution, if it is smaller than 7 add NaOH to increase it.

3. Autoclave the bottle

4. Store at room temperature. If antibiotic needs to be added it should be mixed once the media has cold down around 55 ºC. In that case store in the fridge.

A.2 M63 MINIMAL MEDIA

Preparation of 100 ml of media:

1. Prepare a bottle with 80 ml Milli-Q® Water

2. Add aseptically:

   - 20 ml of 5xM63 salt

   - 100 μl of 1mg/ml B1 stock solution

   - 200 μl of 1M $MgSO_4$

   - 1 ml of 20%w/v glucose

3. Store at room temperature. If antibiotic is added store in the fridge.

A.3 M63 MINIMAL MEDIA SUPPLEMENTED WITH CASAMINO ACIDS

Preparation of 100 ml of media:

1. Prepare a bottle with 80 ml Milli-Q® Water

2. Add aseptically:

   - 20 ml of 5xM63 salt

   - 100 μl of 1mg/ml B1 stock solution

   - 200 μl of 1M $MgSO_4$

   - 1 ml of 20%w/v glucose

   - 1 ml of Casamino acid stock solution 20%

3. Store at room temperature. If antibiotic is added store in the fridge.

A.4 AGAR PLATES

To prepare plates a solidifying agent needs to be added to the nutritional media. In this project the plates were prepared with Agar. The concentration of agar depends on the study that was being perform. Solid plates used to prepare streak plates, require 1.5% agar percentage, is to say 1.5 g of agar per 100 ml of media. Semi-solid plates used for motility assays and three dimensional growth, are in the range of 0.3-0.7% agar (0.3-0.7 g of agar per 100 ml of media).

- To prepare Lysogeny broth plates the appropriate agar concentration is added in the first step with the rest of the components.

  1. Autoclave the bottle

  2. Pour into a petri dish of a desired size. If antibiotic needs to be added it should be mixed once the media has cold down around 55 ºC and then pour into a petri dish of a desired size.

  3. Leave the plates overnight so the condensation will evaporate from the plate and store in the refrigerator

- To prepare plates of Minimal Media the agar is added to the Milli-Q®

  1. Autoclave the bottle

  2. Let to bottle cold down to 55ºC and add the rest of components aseptically, and the antibiotic if required

  3. Leave the plates overnight so the condensation will evaporate from the plate and store in the refrigerator

B

PROTOCOL: P1 TRANSDUCTION

There is no reference for MG1655fliC::kan, also referred as NM109 or ΔfliC, since this is the first project where it is used. It was created by Namiko Mitarai following a transduction method. Protocol: Stanley Brown ad libbed from [59]

MATERIALS

- YT Broth

    - 8g Tryptone (Difco)

    - 5g Yeast Extract (Difco)

    - 5g NaCl

    - 1L H_2O

- H-top Agar: 100 ml H2O, 1g Tryptone, 0.5g NaCl, 0.7g Agar

- Transduction Salts: 20 mM $CaCl_2$ and 10 mM $MgCl_2$

- 1M Trisodium Citrate

- 1M $CaCl_2$

- 1M $MgSO_47H_2O$

- 20% Glucose: filter sterilize

- Donor strain: JW1908-1 from Keio collection [60] obtained from S.L. Svenningsen as a gift.

- Recipient strain: MS613 presented in section 5.1.

METHOD: GROWTH OF DONOR LYSATE

1. Grow donor in YT broth. Dilute fresh overnight 1:10 into 5 ml YT broth containing 0.03 ml 1M CaCl2. Grow 30 - 60 minutes 37℃ on roller or with shaking.

2. In 13 mm test tubes prepare 1 ml aliquots YT broth containing 0 (control for lack of virus infection of bacteria) and 2 or 3 concentrations of between 10^5 to 10^7 PFU of phage P1vir. Add 0.2 - 1 ml aliquots cells and allow phage to adsorb 10 minutes at 37℃ stationary.

3. To each tube add: 0.1 ml 1M CaCl2, 0.2 ml 20% Glucose, YT broth to bring total volume to 2 ml. Mix and add 3 ml molten (50ºC)) H-Top agar after adding agar to each tube, mix immediately and pour on YT agar plate.

4. Incubate overlays at 37ºC, rightside up, 6 - 10 hours

5. When the plate innoculated with the lowest amount of P1 which allows confluent lysis clears, harvest phage by scraping top agar with 3 ml YT broth. Transfer suspension to centrifuge tube containing 0.3 ml 1M MgSO4 and 1 drop CHCl3. Vortex vigorously and clarify (for example, 7K RPM, 5 minutes, Sorvall SS34 rotor). Decant supernatant and filter sterilize. Transfer filtrate to sterile vial and store at 4ºC. The MgSO4 improves the stability of phage P1. Transducing lysates are generally useable for atleast 6 months.

METHOD: TRANSDUCTION OF RECIPIENT

1. Grow recipient in YT broth overnight

2. Harvest freshly saturated culture (for example, 4K RPM, 5 minutes, Sorvall SS34 rotor), decant supernatant, and resuspend cell pellet with 1/2 volume transduction salts.

3. Starve recipients 10 minutes, 37ºC.

4. Adsorb 0.1 ml starved recipients with 0.1 ml of various concentrations of the P1 lysate diluted in YT broth (for example use P1 lysate undiluted, diluted 1:10, and diluted 1:100). It is helpful to include a tube of cells with YT broth added instead of P1 and a tube with the P1 lysate added to the transduction salts and having no cells as controls. Incubate the adsorbtion mixes for 10 minutes at 37ºC.

5. If selected trait is displayed immediately, spread 0.1 ml of the adsorbtion mix on selective agar pre-spread with 0.2 ml 1M sodium citrate per plate. If the selected trait requires time for expression, dilute adsorbtion mixes with 4 ml YT broth containing 50 mM sodium citrate and let grow to express before plating on selective agar pre-spread with 0.2 ml 1M sodium citrate.

6. Restreak transductants the first time on selective agar pre-spread with 0.1 ml 1M sodium citrate. Phage P1 requires Ca++ for adsorbtion, and the citrate protects the transductants from infection by the released P1.

7. Caveat regarding kanamycin-resistance: Citrate protects from killing by kanamycin. Therefore, after growth for sufficient time to allow expression of kanamycin-resistance, and to allow a growth cycle to occur for the P1vir-infected cells, wash the cells a couple of times with the YT-citrate solution, and resuspend them in a small volume of YT-citrate. Then spread the resuspended cells on kanamycin-containing agar without added citrate.

PROTOCOL: TRANSFORMATION

During transformation, specially prepared bacterial cells are given a shock that encourages them to take up foreign DNA. A plasmid typically contains an antibiotic resistance gene, which allows bacteria to survive in the presence of a specific antibiotic. Thus, bacteria that took up the plasmid can be selected on nutrient plates containing the antibiotic. It is important to set controls to be sure that the transformation has been successful.

Protocol: Stanley Brown modified from [61]

MATERIAL

- DNA: pVS130 and pVS132 plasmids

- Mg soln:
    - 10 mM $MgSO_4$
    - 2 mM Tris-HCl pH 7.4

- Ca soln:
    - 50 mM $CaCl_2$
    - 5 mM $MgCl_2$
    - 5 mM NaPIPES pH 6.7 (added aseptically after autoclaving salt soln)

- 0.1 M NaPIPES pH 6.7
    - 1.3 mmoles disodium PIPES (0.456g anhydrous salt)
    - 3.7 mmoles PIPES (1.11g anhydrous acid)
    - H_2O to 50 ml
    - filter sterilize and store at -20°C

- LB 1.5% Agar plates with appropriate antibiotic: 100 $\mu g/ml$ ampicillin

- Streak plate bacterial strain of interest: Δ fliC.

- LB media

CONTROL

Transformation of two different plasmids; 5 control plates:

- Calcium competent cells alone x1

- Calcium competent cells + DNA (x2 one per plasmid)

- $CaCl_2$ solution + DNA (x2 one per plasmid)

METHOD

1. Grow bacteria to early log phase (no higher than 10^8 / ml) in LB, no antibiotic required, since strain of interest present deletion in the genome.

2. Transfer culture to sterile centrifuge tubes

3. Centrifuge 3,000 x g - 5 min - 4°C

4. Decant supernatant and resuspend bacteria by vortexing with 1/2 of the original volume with ice-cold Mg soln.

5. Incubate on ice, 10 - 20 min

6. Centrifuge 2,000 x g - 4 min - 4°C

7. Decant supernatant and resuspend bacteria by vortexing with 1/3 of the original volume with ice-cold Ca soln.

8. Incubate on ice, 20 - 30 min

9. Centrifuge 1,000 x g - 3 min - 4°C

10. Decant supernatant and resuspend bacteria gently with 1/20 - 1/50 of the original volume with ice-cold Ca soln.

11. Mix 200 μl competent cells with 1μl DNA

12. Incubate on ice, 30 - 50 min

13. Perform heat shock, place cells for 60 seconds in 42° water bath

14. Place heat shocked tubes on ice

15. Plate 100 μl immediately since ampicillin is the selection antibiotic of the plasmids.

D

PROTOCOL: MOTILITY ASSAY

Assay to test the ability of different strains to move in different agar concentrations.

MATERIAL

- LB plates of different agar concentrations: 0.3%, 0.4%, 0.5%, 0.6%, 0.7%

- M63 Minimal Media plates of different agar concentrations: 0.3%, 0.4%, 0.5%, 0.6%, 0.7%

- M63 Minimal Media + Casamino acids plates of different agar concentrations: 0.3%, 0.4%, 0.5%, 0.6%, 0.7%

- LB media

- Streak plate bacterial strain of interest: WT, Δfim, Δflu, Δflu Δfim and ΔfliC

METHOD

1. Grow cell culture (3ml) of each strain overnight in LB at 37ºC with shacking

2. Inoculate plates with 1 μl of the saturated culture

3. Incubate plates for 24h at 37ºC

E

PROTOCOL: THREE DIMENSIONAL COLONIES

Protocol to grow three dimensional colonies in semi-solid media of different agar concentrations. Modified from [62].

MATERIAL

- Streak plate bacterial strain of interest: WT, Δfim, Δflu, Δflu Δfim and ΔfliC

- 20 ml mix of Milli-Q® Water and Agar (0.4%, 0.5% or 0.6% as final concentration)

- Ingredients to prepare 25 ml of M63 minimal media:
    - 5 ml of 5xM63 salt
    - 25 μl of 1mg/ml B1 stock solution
    - 50 μl of 1M $MgSO_4$
    - 250 μl of 20%w/v glucose

- LB media

- Ampicillin 100 $\mu g/ml$

- IPTG 1mM

- Glass bottomed dish

METHOD

1. Grow cell culture (3ml) of the strain overnight in LB at 37ºC with shacking

2. Turn on the block heater and set it up to 55ºC, to ensure an uniform heating of the sample fill the holes with water.

3. Place as many 1.5 ml eppendorf tubes as final plates we want to have at the heater.

4. Heat the 20 ml mix of Milli-Q® Water and Agar in the microwave until the agar is completely melted. Heat in short periods of time and move the mix to see if any solid agar regions remain.

5. Wait until the 20 ml mix of Milli-Q® Water and melted agar is cold enough to add the rest of components to prepare M63 minimal media.

6. Place 1 ml of M63 minimal media with agar in each of the heater eppendorf tubes.

7. Remove overnight culture and measure its OD600.

8. Perform three step serial dilution of the overnight culture. Usually 10 μl of the overnight are mixed with 1 ml of LB media, but the volume taken from the overnight can change depending on its OD600 value. Then take 10 μl of the first dilution and mix with 1 ml of LB media. Lastly take 10 μl of the second dilution and mix with 1 ml of LB media.

9. Add 5 μl IPTG and 1 μl of ampicillin into one of the heater eppendorf tubes.

10. Add 10 μl of the last bacterial dilution into the same eppendorf tube, quickly mix the content and pour it into a glass bottomed dish.

11. Let the agar solidify for approx. 5 min and put the dish into the incubator at 37ºC for as long as desired, usually 15 h.

OPTICAL DENSITY

Protocol to measure the OD600, optical density at 600 nm wavelength, of a liquid culture in order to estimate the number of bacteria in it.

MATERIALS

- NanoPhotometer (N120/NP80/N60/N50/C40)

- Cuvette

- Liquid culture

- Same media as the liquid culture

METHOD

1. Turn on spectrophotometer and select OD600 and cuvette application.

2. Fill one cuvette with 550 μl of media, insert it in the spectrophotometer and take the blank measure.

3. Fill one cuvette with 500 μl of media and 50 μl of the liquid culture, insert it in the spectrophotometer and take a sample.

4. Write down the OD600 value and compute the number of cells in the sample, in *E.coli*:

$$cells/ml = OD600 \cdot 5 \cdot 10^8 cells/ml \qquad (20)$$

Since the sample has been diluted the actual number of cells is ten times the result of the previous expression. The cell factor was obtained from [63]. Even though to know the exact number of cells in a particular media a calibration curve needs to be measured this factor is considered appropriated to our study. That is because we look at saturated samples and a high precision is not required since the order of magnitude obtained with this protocol is correct.

DISTRIBUTIONS AT 0.5% AGAR CONCENTRATION
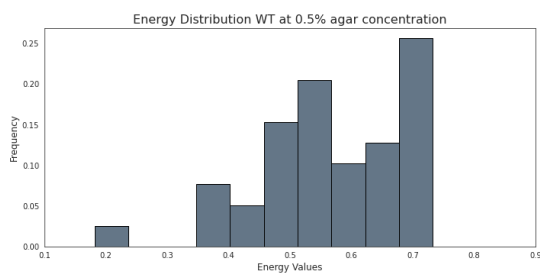
ENERGY

Figure 41: Energy distribution of WT at 0.5% agar concentration
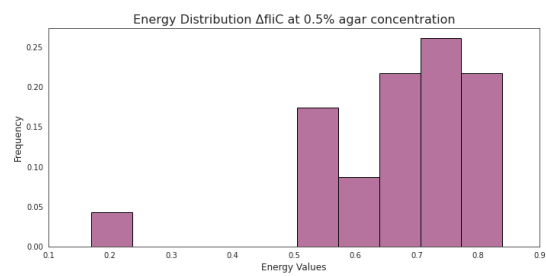
Figure 42: Energy distribution of ΔfliC at 0.5% agar concentration
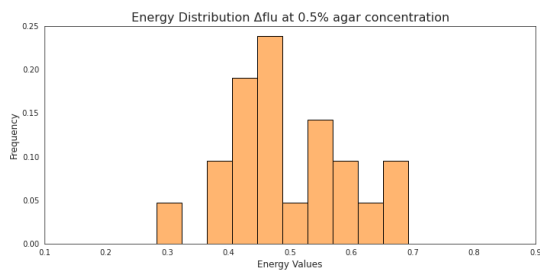
Figure 43: Energy distribution of Δflu at 0.5% agar concentration
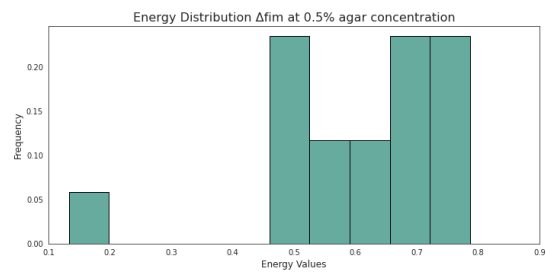
Figure 44: Energy distribution of Δfim at 0.5% agar concentration
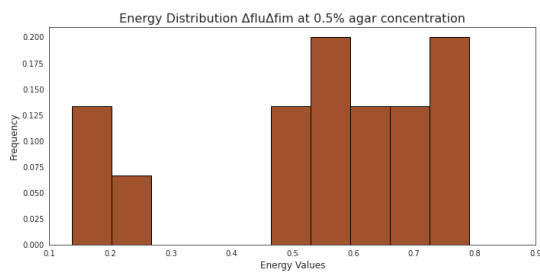
Figure 45: Energy distribution of ΔfluΔfim at 0.5% agar concentration

Distribution of textural energy for different bacterial strains, the x-axe is fixed between 0.1 and 0.9 and the histograms are normalized. The distributions of Δfim and ΔfluΔfim look more uniform than normal.

ENTROPY
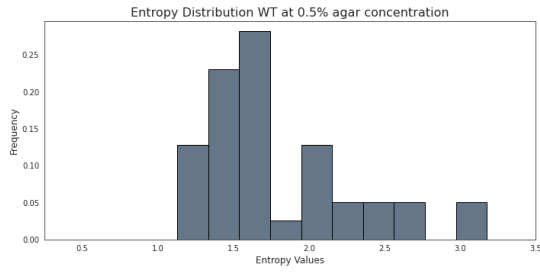
Figure 46: Entropy distribution of WT at 0.5% agar
concentration
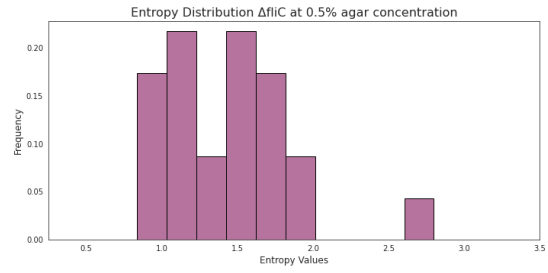
Figure 47: Entropy distribution of ΔfliC at 0.5%
agar concentration
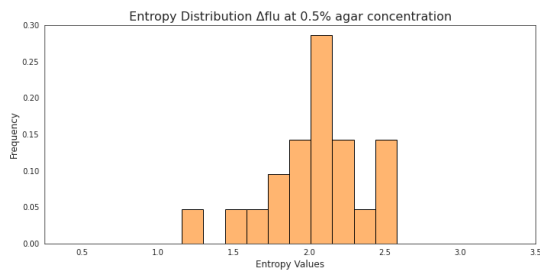
Figure 48: Entropy distribution of Δflu at 0.5% agar
concentration
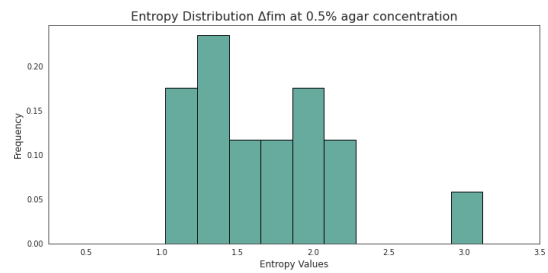
Figure 49: Entropy distribution of Δfim at 0.5% agar
concentration
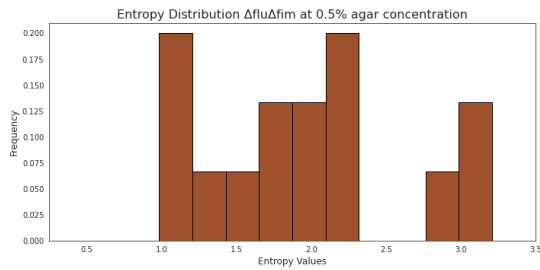
Figure 50: Entropy distribution of ΔfluΔfim at 0.5%
agar concentration

Distribution of textural entropy for different bacterial strains, the x-axe is fixed between 0.25 and 3.5 and the histograms are normalized. The distributions of Δfim and ΔfluΔfim look more uniform than normal.

HOMOGENEITY
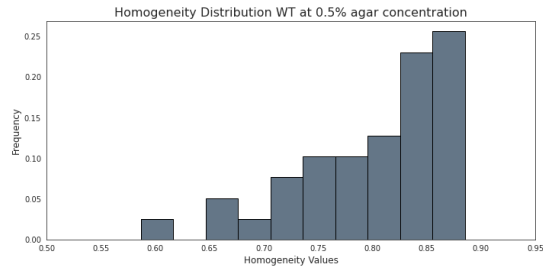
Figure 51: Homogeneity distribution of WT at 0.5% agar concentration
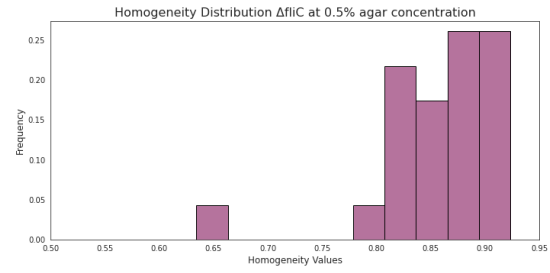
Figure 52: Homogeneity distribution of ΔfliC at 0.5% agar concentration
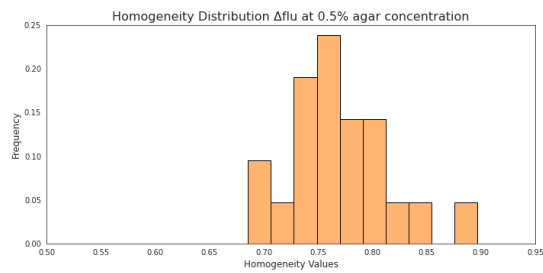
Figure 53: Homogeneity distribution of Δflu at 0.5% agar concentration
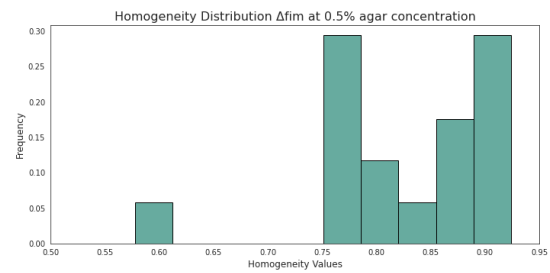
Figure 54: Homogeneity distribution of Δfim at 0.5% agar concentration
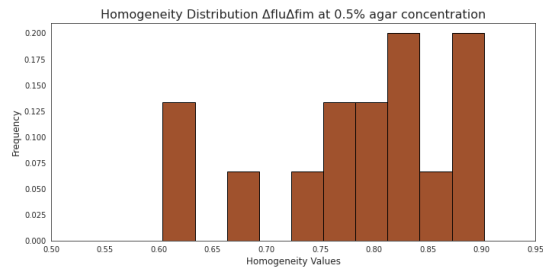
Figure 55: Homogeneity distribution of ΔfluΔfim at 0.5% agar concentration

Distribution of textural homogeneity for different bacterial strains, the x-axe is fixed between 0.5 and 0.95 and the histograms are normalized. The distributions of Δfim and ΔfluΔfim look more uniform than normal.

ASPECT RATIO
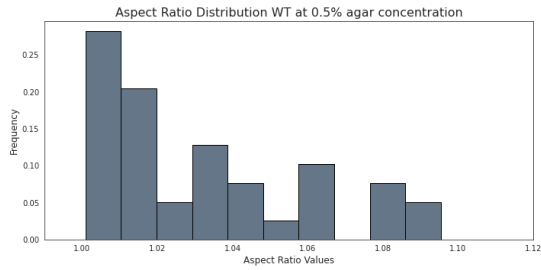
Figure 56: Aspect Ratio distribution of WT at 0.5% agar concentration
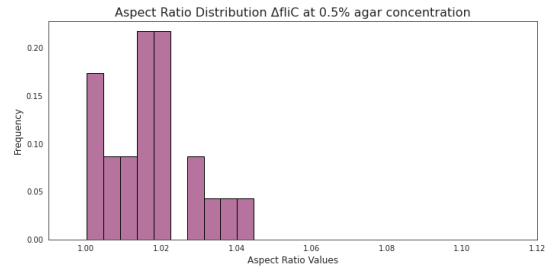
Figure 57: Aspect Ratio distribution of ΔfliC at 0.5% agar concentration
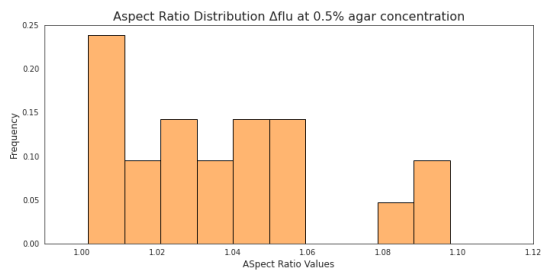
Figure 58: Aspect Ratio distribution of Δflu at 0.5% agar concentration
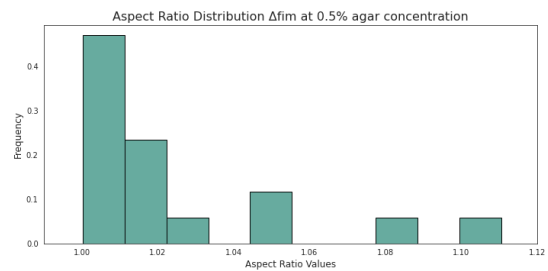
Figure 59: Aspect Ratio distribution of Δfim at 0.5% agar concentration
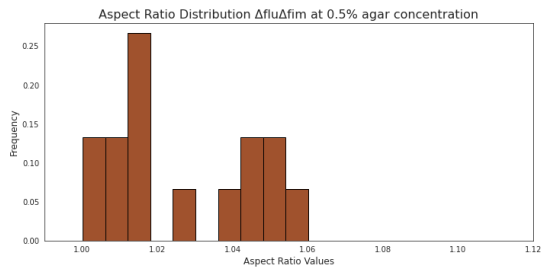
Figure 60: Aspect Ratio distribution of ΔfluΔfim at 0.5% agar concentration

Distribution of aspect ratios for different bacterial strains, the x-axe is fixed between 0.99 and 1.12 and the histograms are normalized. All of them look quite normal but ΔfliC and ΔfluΔfim seem to have its center displaced from one, the value that describe spherical colonies.

FRACTAL DIMENSION
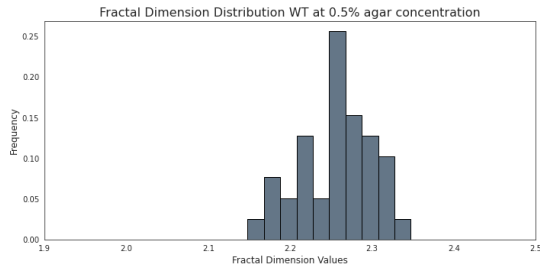
Figure 61: Fractal Dimension distribution of WT at 0.5% agar concentration
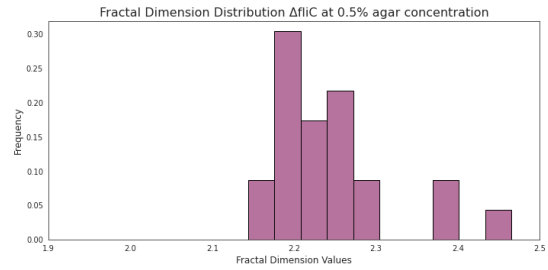
Figure 62: Fractal Dimension distribution of ΔfliC at 0.5% agar concentration
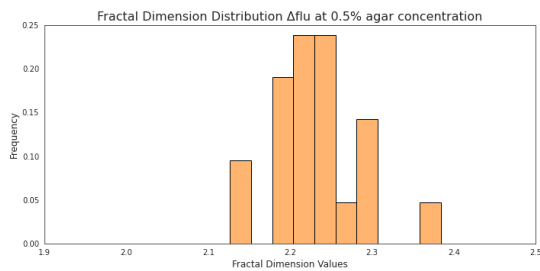
Figure 63: Fractal Dimension distribution of Δflu at 0.5% agar concentration
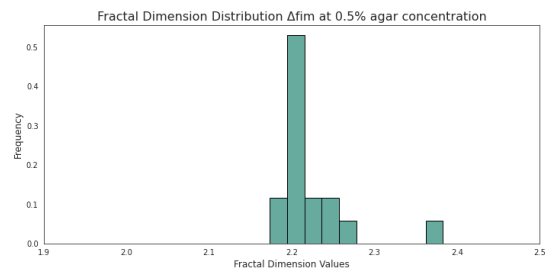
Figure 64: Fractal Dimension distribution of Δfim at 0.5% agar concentration
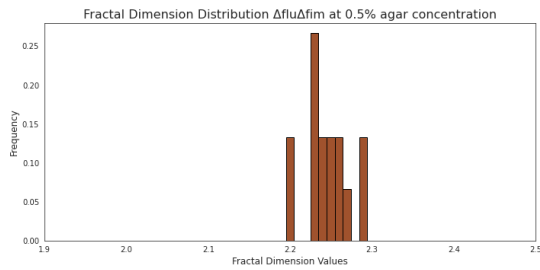
Figure 65: Fractal Dimension distribution of ΔfluΔfim at 0.5% agar concentration

Distribution of fractal dimension for different bacterial strains, the x-axe is fixed between 1.9 and 2.5 and the histograms are normalized. All of them look quite normal.

T-VALUES

TEST BETWEEN STRAINS AT 0.4% AGAR CONCENTRATION

	Energy		Entropy		Homogeneity	
	T_{val}	p_{val}	T_{val}	p_{val}	T_{val}	p_{val}
ΔfliC / Δflu	8.14	0.0001152	-7.380	0.000160	7.32	0.00021
ΔfliC / Δfim	36.28	1.2508e-09	-26.477	4.95e-09	22.406	1.1e-09
ΔfliC / ΔfluΔfim	11.682	1.532e-07	-9.721	1.0812e-06	11.205	2.851e-07
Δflu / Δfim	1.172	0.2836	-1.539	0.170	1.18	0.273
Δflu / ΔfluΔfim	-3.93	0.0056	3.26	0.013	-3.66	0.0085
Δfim / ΔfluΔfim	16.216	1.24e-08	12.80	3.85e-08	-12.296	4.689e-08

Table 11: Table showing the T_{val} and p_{val} of the quantified textural parameters for the colonies growing at 0.6% agar concentration. This results are analyzed under a significance of $\alpha = 5\%$. WT strain not included since experimental colonies observed were not comparable to rest of strains

	Aspect Ratio		Fractal dimension	
	T_{val}	p_{val}	T_{val}	p_{val}
ΔfliC / Δflu	-2.217	0.06248	1.416	0.199
ΔfliC / Δfim	-0.115	0.910	0.1069	0.9169
ΔfliC / ΔfluΔfim	-0.9584	0.361	0.8429	0.422
Δflu / Δfim	2.138	0.0681	-0.924	0.381
Δflu / ΔfluΔfim	1.400	0.190	0.3082	0.766
Δfim / ΔfluΔfim	-0.8566	0.41066	0.736	0.477

Table 12: Table showing the T_{val} and p_{val} of the quantified volumetric parameters for the colonies growing at 0.6% agar concentration. This results are analyzed under a significance of $\alpha = 5\%$. WT strain not included since experimental colonies observed were not comparable to rest of strains

TEST BETWEEN STRAINS AT 0.6% AGAR CONCENTRATION

	Energy		Entropy		Homogeneity	
	T_{val}	p_{val}	T_{val}	p_{val}	T_{val}	p_{val}
WT / ΔfliC	-0.464	0.66	0.944	0.374	-0.9199	0.393
WT / Δflu	1.45	0.189	1.281	0.240	-3.0225	0.0282
WT / Δfim	-2.428	0.036	3.173	0.0104	-2.814	0.0183
WT / ΔfluΔfim	-8.246	4.22e-05	4.80	0.0019	-7.109	0.000102
ΔfliC / Δflu	-0.224	0.831	0.107	0.917	-0.609	0.572
ΔfliC / Δfim	-1.0383	0.33	1.78	0.11	-1.0648	0.32
ΔfliC / ΔfluΔfim	-3.5431	0.017	3.5	0.0074	-3.577	0.012
Δflu / Δfim	-1.46	0.1795	2.056	0.0716	-0.960	0.3682
Δflu / ΔfluΔfim	-7.64	0.000129	3.971	0.00666	-6.380	0.0011
Δfim / ΔfluΔfim	-3.805	0.00411	2.31	0.0517	-3.390	0.00691

Table 13: Table showing the T_{val} and p_{val} of the quantified textural parameters for the colonies growing at 0.6% agar concentration. This results are analyzed under a significance of $\alpha = 5\%$.

	Aspect Ratio		Fractal dimension	
	T_{val}	p_{val}	T_{val}	p_{val}
WT / ΔfliC	0.467	0.653	-1.258	0.247
WT / Δflu	-1.9051	0.1225	0.7465	0.490
WT / Δfim	-0.0804	0.937	-0.6050	0.5590
WT / ΔfluΔfim	-0.249	0.812	-1.3042	0.2309
ΔfliC / Δflu	-2.127	0.085	3.0182	0.0264
ΔfliC / Δfim	-0.4545	0.659	0.538	0.6025
ΔfliC / ΔfluΔfim	-0.520	0.621	-0.095	0.926
Δflu / Δfim	1.646	0.1486	-1.5349	0.168
Δflu / ΔfluΔfim	1.189	0.272	-2.949	0.0299
Δfim / ΔfluΔfim	-0.1755	0.865	-0.60	0.56

Table 14: Table showing the T_{val} and p_{val} of the quantified volumetric parameters for the colonies growing at 0.6% agar concentration. This results are analyzed under a significance of $\alpha = 5\%$.

TEST BETWEEN SAME STRAIN AT DIFFERENT AGAR CONCENTRATION

WT						
	Energy		Entropy		Homogeneity	
	T_{val}	p_{val}	T_{val}	p_{val}	T_{val}	p_{val}
0.5% / 0.6%	6.77	1.5e-4	-5.11	0.00048	5.64	0.00022

ΔfliC						
	Energy		Entropy		Homogeneity	
	T_{val}	p_{val}	T_{val}	p_{val}	T_{val}	p_{val}
0.4% / 0.5%	6.13	2.2e-6	-7.41	7.49e-8	5.53	8.5e-6
0.4% / 0.6%	6.26	3.1e-3	-11.074	0.000144	7.05	0.00179
0.5% / 0.6%	3.6	0.014	-5.28	0.00081	4.189	0.0066

Δflu						
	Energy		Entropy		Homogeneity	
	T_{val}	p_{val}	T_{val}	p_{val}	T_{val}	p_{val}
0.4% / 0.5%	1.28	0.22	-1.066	0.313	0.454	0.659
0.4% / 0.6%	3.89	0.0036	-2.41	0.039	1.721	0.129
0.5% / 0.6%	3.48	0.007	-2.0635	0.075	2.074	0.050

Δfim						
	Energy		Entropy		Homogeneity	
	T_{val}	p_{val}	T_{val}	p_{val}	T_{val}	p_{val}
0.4% / 0.5%	-2.52	0.022	3.440	0.0029	-3.117	0.00573
0.4% / 0.6%	1.16	0.28	0.899	0.398	-0.384	0.7112
0.5% / 0.6%	2.55	0.022	-2.11	0.0469	2.192	0.04060

ΔfluΔfim						
	Energy		Entropy		Homogeneity	
	T_{val}	p_{val}	T_{val}	p_{val}	T_{val}	p_{val}
0.4% / 0.5%	2.78	0.014	-3.169	0.0058	2.851	0.0120
0.4% / 0.6%	1.68	0.148	-1.256	0.2667	1.053	0.3399
0.5% / 0.6%	-1.78	0.091	1.55	0.1416	-1.957	0.0660

Table 15: Table showing the T_{val} and p_{val} of the quantified textural parameters for the colonies growing at different agar concentrations. This results are analyzed under a significance of $\alpha = 5\%$.

WT				
	Aspect Ratio		Fractal Dimension	
	T_{val}	p_{val}	T_{val}	p_{val}
0.5% / 0.6%	-0.807	0.44	0.973	0.379

ΔfliC				
	Aspect Ratio		Fractal Dimension	
	T_{val}	p_{val}	T_{val}	p_{val}
0.4% / 0.5%	-1.78	0.10	-0.4084	0.688
0.4% / 0.6%	-2.27	0.073	-1.364	0.212
0.5% / 0.6%	-1.60	0.17	-0.985	0.34

Δflu				
	Aspect Ratio		Fractal Dimension	
	T_{val}	p_{val}	T_{val}	p_{val}
0.4% / 0.5%	-0.017	0.98	-1.339	0.193
0.4% / 0.6%	-1.871	0.11	0.59	0.568
0.5% / 0.6%	-2.12	0.1012	1.858	0.081

Δfim				
	Aspect Ratio		Fractal Dimension	
	T_{val}	p_{val}	T_{val}	p_{val}
0.4% / 0.5%	-1.553	0.134	0.4933	0.633
0.4% / 0.6%	-2.36	0.048	-0.482	0.638
0.5% / 0.6%	-1.137	0.278	-0.944	0.373

ΔfluΔfim				
	Aspect Ratio		Fractal Dimension	
	T_{val}	p_{val}	T_{val}	p_{val}
0.4% / 0.5%	-0.93	0.36	-1.0566	0.323
0.4% / 0.6%	-1.34	0.23	-1.562	0.149
0.5% / 0.6%	-0.957	0.385	-1.27	0.260

Table 16: Table showing the T_{val} and p_{val} of the quantified volumetric parameters for the colonies growing at different agar concentrations. This results are analyzed under a significance of $\alpha = 5\%$.

BIBLIOGRAPHY

[1] M. Ohgiwari, M. Matsushita, and T. Matsuyama, "Morphological Changes in Growth Phenomena of Bacterial Colony Patterns", Journal of the Physical Society of Japan **61**, Publisher: The Physical Society of Japan, 816–822 (1992).

[2] L. Huang and T. Wu, "Novel neural network application for bacterial colony classification", en, Theoretical Biology and Medical Modelling **15**, 22 (2018).

[3] A. M. Sousa, I. Machado, A. Nicolau, and M. O. Pereira, "Improvements on colony morphology identification towards bacterial profiling", en, Journal of Microbiological Methods **95**, 327–335 (2013).

[4] M. Mimura, H. Sakaguchi, and M. Matsushita, "Reaction–diffusion modelling of bacterial colony patterns", en, Physica A: Statistical Mechanics and its Applications **282**, 283–303 (2000).

[5] P.-T. Su, C.-T. Liao, J.-R. Roan, S.-H. Wang, A. Chiou, and W.-J. Syu, "Bacterial Colony from Two-Dimensional Division to Three-Dimensional Development", en, PLoS ONE **7**, edited by A. Driks, e48098 (2012).

[6] S. M. Soto, "Role of efflux pumps in the antibiotic resistance of bacteria embedded in a biofilm", eng, Virulence **4**, 223–229 (2013).

[7] C. Potera, "Forging a link between biofilms and disease", eng, Science (New York, N.Y.) **283**, 1837, 1839 (1999).

[8] P. Smadbeck and M. P. Stumpf, "Coalescent models for developmental biology and the spatio-temporal dynamics of growing tissues", en, bioRxiv, Publisher: Cold Spring Harbor Laboratory Section: New Results, 022251 (2015).

[9] P. H. Rampelotto, "Extremophiles and Extreme Environments", Life : Open Access Journal **3**, 482–485 (2013).

[10] R. M. Maier, "Chapter 3 - Bacterial Growth", en, in *Environmental Microbiology (Second Edition)*, edited by R. M. Maier, I. L. Pepper, and C. P. Gerba (Academic Press, San Diego, Jan. 2009), pp. 37–54.

[11] S. Humagain, "Growth of bacteria and the bacterial growth curve", en-US, Online Science Notes (2018).

[12] K. F. Jarrell and M. J. McBride, "The surprisingly diverse ways that prokaryotes move", en, Nature Reviews Microbiology **6**, 466–476 (2008).

[13] D. F. Blair, "How bacteria sense and swim", eng, Annual Review of Microbiology **49**, 489–522 (1995).

[14] J.-M. Swiecicki, O. Sliusarenko, and D. B. Weibel, "From swimming to swarming: Escherichia coli cell motility in two-dimensions", Integrative biology : quantitative biosciences from nano to macro **5**, 1490–1494 (2013).

[15] G. A. O'Toole and R. Kolter, "Flagellar and twitching motility are necessary for Pseudomonas aeruginosa biofilm development", en, Molecular Microbiology **30**, 295–304 (1998).

[16] J. Tchoufag, P. Ghosh, C. B. Pogue, B. Nan, and K. K. Mandadapu, "Mechanisms for bacterial gliding motility on soft substrates", en, Proceedings of the National Academy of Sciences **116**, Publisher: National Academy of Sciences Section: Biological Sciences, 25087–25096 (2019).

[17] T. Hölscher and Á. T. Kovács, "Sliding on the surface: bacterial spreading without an active motor", en, Environmental Microbiology **19**, 2537–2545 (2017).

[18] F. C. Neidhardt and S. R. Kushner, "Escherichia coli", en, in *Reference Module in Life Sciences* (Elsevier, Jan. 2017).

[19] B. J. Bachmann, "Derivations and Genotypes of Some Mutant Derivatives of Escherichia coli K-12", en, In: Neidhardt et al., eds., 37.

[20] J.-A. Conchello and J. W. Lichtman, "Optical sectioning microscopy", en, Nature Methods **2**, 920–931 (2005).

[21] M. J. Sanderson, I. Smith, I. Parker, and M. D. Bootman, "Fluorescence Microscopy", en, Cold Spring Harbor Protocols **2014**, pdb.top071795–pdb.top071795 (2014).

[22] J. Jonkman, C. M. Brown, G. D. Wright, K. I. Anderson, and A. J. North, "Tutorial: guidance for quantitative confocal microscopy", en, Nature Protocols **15**, 1585–1611 (2020).

[23] T. J. Fellers and M. W. Davidson, "Confocal Microscopy - Introduction — Olympus LS", Introduction to Confocal Microscopy.

[24] ZEISS, "LSM 900 for Materials", en, The Confocal Principle.

[25] H. Beyenal, Z. Lewandowski, and G. Harkin, "Quantifying biofilm structure: facts and fiction", eng, Biofouling **20**, 1–23 (2004).

[26] H. Beyenal, C. Donovan, Z. Lewandowski, and G. Harkin, "Three-dimensional biofilm structure quantification", Journal of microbiological methods **59**, 395–413 (2005).

[27] R. M. Haralick, K. Shanmugam, and I. Dinstein, "Textural Features for Image Classification", IEEE Transactions on Systems, Man, and Cybernetics **SMC-3**, Conference Name: IEEE Transactions on Systems, Man, and Cybernetics, 610–621 (1973).

[28] K. Falconer, *Fractal Geometry: Mathematical Foundations and Applications*, en (John Wiley & Sons, Dec. 2013).

[29] B. Dubuc, S. W. Zucker, C. Tricot, J. F. Quiniou, and D. Wehbi, "Evaluating the Fractal Dimension of Surfaces", Proceedings of the Royal Society of London. Series A, Mathematical and Physical Sciences **425**, Publisher: The Royal Society, 113–127 (1989).

[30] D. Kalpić, N. Hlupić, and M. Lovrić, "Student's t-Tests", en, in *International Encyclopedia of Statistical Science*, edited by M. Lovric (Springer, Berlin, Heidelberg, 2011), pp. 1559–1563.

[31] Z. Lu and K.-H. Yuan, "Welch's t test", 1620–1623 (2010).

[32] F. R. Blattner, G. Plunkett, C. A. Bloch, N. T. Perna, V. Burland, M. Riley, J. Collado-Vides, J. D. Glasner, C. K. Rode, G. F. Mayhew, J. Gregor, N. W. Davis, H. A. Kirkpatrick, M. A. Goeden, D. J. Rose, B. Mau, and Y. Shao, "The Complete Genome Sequence of Escherichia coli K-12", en, Science **277**, Publisher: American Association for the Advancement of Science Section: Articles, 1453–1462 (1997).

[33] L. Jauffred, R. Munk Vejborg, K. S. Korolev, S. Brown, and L. B. Oddershede, "Chirality in microbial biofilms is mediated by close interactions between the cell surface and the substratum", en, The ISME Journal **11**, Number: 7 Publisher: Nature Publishing Group, 1688–1701 (2017).

[34] K. Kjaergaard, M. A. Schembri, C. Ramos, S. Molin, and P. Klemm, "Antigen 43 facilitates formation of multispecies biofilms", eng, Environmental Microbiology **2**, 695–702 (2000).

[35] A. Reisner, J. A. J. Haagensen, M. A. Schembri, E. L. Zechner, and S. Molin, "Development and maturation of Escherichia coli K-12 biofilms", en, Molecular Microbiology **48**, 933–946 (2003).

[36] I. R. Henderson, M. Meehan, and P. Owen, "Antigen 43, a phase-variable bipartite outer membrane protein, determines colony morphology and autoaggregation in Escherichia coli K-12", FEMS Microbiology Letters **149**, 115–120 (1997).

[37] J. D. Schilling, M. A. Mulvey, and S. J. Hultgren, "Structure and Function of Escherichia coli Type 1 Pili: New Insight into the Pathogenesis of Urinary Tract Infections", The Journal of Infectious Diseases **183**, S36–S40 (2001).

[38] S. Nakamura and T. Minamino, "Flagella-Driven Motility of Bacteria", Biomolecules **9**, `10.3390/biom9070279` (2019).

[39] F. Mayer, "Role of Elongation Factor EF-Tu in Bacterial Cytoskeletons - Mini Review and Update", Swift Journal of Medicine and Medical Sciences **Vol. 1 (2)**, 06–011 (2015).

[40] H. Hasman, T. Chakraborty, and P. Klemm, "Antigen-43-Mediated Autoaggregation of Escherichia coli Is Blocked by Fimbriation", Journal of Bacteriology **181**, 4834–4841 (1999).

[41] V. M. Suchanek, M. Esteban-López, R. Colin, O. Besharova, K. Fritz, and V. Sourjik, "Chemotaxis and cyclic-di-GMP signalling control surface attachment of Escherichia coli", en, Molecular Microbiology **113**, 728–739 (2020).

[42] C. E. Bell and M. Lewis, "A closer view of the conformation of the Lac repressor bound to operator", eng, Nature Structural Biology **7**, 209–214 (2000).

[43] A. J. Mitchell and J. W. Wimpenny, "The effects of agar concentration on the growth and morphology of submerged colonies of motile and non-motile bacteria", eng, Journal of Applied Microbiology **83**, 76–84 (1997).

[44] "Fluorescence SpectraViewer", en, https://www.thermofisher.com/order/fluorescence-spectraviewer.

[45] J. Schindelin, *Fiji: an open-source platform for biological-image analysis*, Vol. 9(7), Pages: 676-682 (2012).

[46] N. Otsu, "A Threshold Selection Method from Gray-Level Histograms", IEEE Transactions on Systems, Man, and Cybernetics **9**, Conference Name: IEEE Transactions on Systems, Man, and Cybernetics, 62–66 (1979).

[47] "3D ImageJ Suite", en, ImageJ,https://imagej.net/3D_ImageJ_Suite.

[48]"Process Menu", https://imagej.nih.gov/ij/docs/menus/process.html.

[49]B. Schmid, "A high-level 3D visualization API for Java and ImageJ", Bmcbioinformatics **11(1)** (2010).

[50]G. C. Ulett, R. I. Webb, and M. A. 2. Schembri, "Antigen-43-mediated autoaggregation impairs motility in Escherichia coli", Microbiology **152**, Publisher: Microbiology Society, 2101–2110.

[51]N. Kandemir, W. Vollmer, N. S. Jakubovics, and J. Chen, "Mechanical interactions between bacteria and hydrogels", en, Scientific Reports **8**, Number: 1 Publisher: Nature Publishing Group, 10893 (2018).

[52]M. Cordero, "Full data set", https://sid.erda.dk/cgi-sid/ls.py?share_id=aCt7mMRoOX.

[53]M. M. Larsen, "Master's theses", en, NBI Master's theses (2021).

[54]M. Eden, "A Two-dimensional Growth Process", Proceedings of the Fourth Berkeley Symposium on Mathematical Statistics and Probability, Volume 4: Contributions to Biology and Problems of Medicine, Publisher: University of California Press, 223–239 (1961).

[55]M. T. Batchelor and B. I. Henry, "Limits to Eden growth in two and three dimensions", en, Physics Letters A **157**, 229–236 (1991).

[56]E. W. Kuennen and C. Y. Wang, "Off-lattice radial Eden cluster growth in two and three dimensions", en, Journal of Statistical Mechanics: Theory and Experiment **2008**, Publisher: IOP Publishing, P05014 (2008).

[57]J. Tailleur and M. E. Cates, "Statistical Mechanics of Interacting Run-and-Tumble Bacteria", Physical Review Letters **100**, Publisher: American Physical Society, 218103 (2008).

[58]"ECMDB: ECMDB Statistics", Escherichia coli Statistics.

[59]H. Malke, "T. J. Silhavy, M. L. Berman and L. W. Enquist (Editors), Experiments with Gene Fusions. 303 S., 32 Abb., 11 Tab. Cold Spring Harbor 1984. Cold Spring Harbor Laboratory. $ 48.00. ISBN: 0-87969-163-8", en, Journal of Basic Microbiology **25**, 350–350 (1985).

[60]"Strain - JW1908-1", https://cgsc.biology.yale.edu/Strain.php?ID=107867.

[61]S. N. Cohen, A. C. Y. Chang, and L. Hsu, "Nonchromosomal Antibiotic Resistance in Bacteria: Genetic Transformation of Escherichia coli by R-Factor DNA*", Proceedings of the National Academy of Sciences of the United States of America **69**, 2110–2114 (1972).

[62]R. S. Eriksen, N. Mitarai, and K. Sneppen, "On Phage Adsorption to Bacterial Chains", en, Biophysical Journal **119**, 1896–1904 (2020).

[63]"IMPLEN NanoPhotometer ® N120/NP80/N60/N50/C40 User Manual", User Manual.